

NASA CR-54276

THIRD QUARTERLY REPORT PRESSURE MEASURING SYSTEMS FOR CLOSED CYCLE LIQUID METAL FACILITIES

Anthony J. Cassano

GPO PRICE \$ _____

OTS PRICE(S) \$ _____

Hard copy (HC) 3.00

Microfiche (MF) .75

PREPARED FOR
NATIONAL AERONAUTICS AND SPACE ADMINISTRATION
CONTRACT NAS 3-4170

December 28, 1964

FACILITY FORM 902	N 65 15350	
	(ACCESSION NUMBER)	(THRU)
	72	1
	(PAGES)	(CODE)
	CP 54276	14
	(NASA CR OR TMX OR AD NUMBER)	(CATEGORY)

CONSOLIDATED CONTROLS CORP.
BETHEL, CONNECTICUT



NOTICE

This report was prepared as an account of Government sponsored work. Neither the United States, nor the National Aeronautics and Space Administration (NASA), nor any person acting on behalf of NASA:

- A.) Makes any warranty or representation, expressed or implied, with respect to the accuracy, completeness, or usefulness of the information contained in this report, or that the use of any information, apparatus, method, or process disclosed in this report may not infringe privately owned rights; or
- B.) Assumes any liabilities with respect to the use of, or for damages resulting from the use of any information, apparatus, method or process disclosed in this report.

As used above, "person acting on behalf of NASA" includes any employee or contractor of NASA, or employee of such contractor, to the extent that such employee or contractor of NASA, or employer of such contractor prepares, disseminates, or provides access to, any information pursuant to his employment or contract with NASA, or his employment with such contractor.

Requests for copies of this report should be referred to:

National Aeronautics and Space Administration
Office of Scientific and Technical Information
Washington, D. C. 20546
Attention: AFSS-A

CASE FILE COPY

THIRD QUARTERLY REPORT
September 1--November 30, 1964

PRESSURE MEASURING SYSTEMS
FOR
CLOSED CYCLE LIQUID METAL FACILITIES

PREPARED FOR
NATIONAL AERONAUTICS AND SPACE ADMINISTRATION

CONTRACT NAS 3-4170

DECEMBER 28, 1964

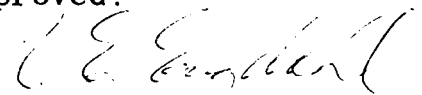
Technical Management
NASA - Lewis Research Center
Nuclear Power Technology Branch
R. N. Weltmann

Prepared by:



Anthony J. Cassano
Research Engineer

Approved:



R. E. Engdahl
Project Manager

Consolidated Controls Corporation
Bethel, Connecticut

FOREWORD

The major contributors to this development program are Mr. R. Engdahl, Project Manager, Mr. Anthony Cassano and Mr. David Mends.

ABSTRACT

15350

Continuing development of a pressure transducer system for liquid metal applications is described. During the report period, emphasis was on the experimental program and the following results are presented: (1) pressure-deflection-temperature characteristics of pressure capsules of FS-85 and W-25Re alloys, (2) current-spacing characteristics of the latest thermionic diode sensor, (3) Q-meter data on the variable impedance sensor, and (4) life test data on a representative electrical terminal. Design configurations are presented for potassium compatibility testing of the pressure capsules and the electrical terminal.

Authas →

TABLE OF CONTENTS

<u>Section</u>	<u>Title</u>	<u>Page No.</u>
	Abstract	i
	Table of Contents	ii
	List of Illustrations	iii
1.0	Introduction	1
2.0	Summary	3
3.0	Pressure Capsule	5
3.1	Test Results	7
4.0	Deflection-Electrical Signal	11
4.1	Thermionic Diode Sensor	13
4.1.1	Test Results	16
4.2	Variable Impedance Sensor	19
4.2.1	Test Results	20
5.0	Electrical Terminal	23
6.0	Vacuum Test Facility	25
6.1	Liquid Potassium Compatibility	26
6.2	Diaphragm Deflection Measurement	29
	References	58
	Appendix A - Nomenclature	59

LIST OF ILLUSTRATIONS

<u>Number</u>	<u>Title</u>	<u>Page No.</u>
1.	FS-85 Pressure Deflection; Room Temperature	32
2.	FS-85 Pressure Deflection; 500°F	33
3.	" " " 1000°F	34
4.	" " " 1400°F	35
5.	" " " 1800°F	36
6.	W-25Re Pressure Deflection; Room Temperature	37
7.	W-25Re Pressure Deflection; 500°F	38
8.	" " " 1000°F	39
9.	" " " 1200°F	40
10.	" " " 1400°F	41
11.	" " " 1600°F	42
12.	" " " 1800°F	43
13.	Full Scale Deflection-Temperature Characteristics	44
14.	Dual Emitter Test Device	45
15.	Dual Emitter Test Device; Vacuum Chamber Installation	46
16a.	Thermionic Test Circuitry	47
16b.	" " "	47

LIST OF ILLUSTRATIONS (Cont'd)

<u>Number</u>	<u>Title</u>	<u>Page No.</u>
17.	Current-Distance Characteristics; Thermionic Sensor at 1800°F	48
18.	Inductance-Distance Characteristics; Copper Diaphragm	49
19.	Inductance-Distance Characteristics; Cupronickel Diaphragm	50
20.	Inductance-Distance Characteristics; FS-85, Monel and K-Monel Diaphragms	51
21.	Electrical Terminal Life Test Configuration	52
22.	Ion Pump Installation	53
23.	Compatibility Test Design for Columbium and Tantalum Capsules	54
24.	Compatibility Test Design for W-25Re Capsule	55
25.	Compatibility Test Design for Electrical Terminals	56
26.	Typical Metallographic Plate	57

1.0 Introduction

The objective of Contract NAS 3-4170 is to develop pressure transducer equipment compatible with advanced closed cycle power systems. The systems utilize liquid metals such as mercury, sodium, potassium and other alkali metals as working and heat transfer media at elevated temperatures. Pressure measurements in the high temperature liquid, vapor, and two phase streams will be required for research, design and control purposes for SNAP-8 and other liquid metal space power systems. Since small pressure changes might indicate the onset of instability, instruments are required that can follow and record minute changes. In addition, space flight requires light-weight systems capable of enduring long periods of unattended operation.

Liquid metal pressure measurements at elevated temperatures pose many problems which challenge the designer and demand the best from available materials. To establish a firm design base for

the transducer equipment, four materials and two transducer systems have been chosen for evaluation. The selected material and transduction system will be developed for use as either ground or flight hardware.

2.0 Summary

Progress in the design, fabrication and testing of the FS-85, C129Y and W-25 Re pressure capsules is presented. Capsules have been successfully fabricated from FS-85, C-129Y and W-25Re (ring and disc design). Spark discharge machining is presently being done to prepare discs of W-25Re. Complete pressure-deflection-temperature tests have been performed on the FS-85 (0.004 inch maximum deflection) and the W-25Re (0.002 inch maximum deflection) capsules. Results of these tests are presented. Tests on the W-25Re (0.004 inch maximum deflection) and the C-129Y (0.002 inch maximum deflection) capsules are in their final stages.

An improved experimental thermionic diode sensor has been designed and built, and preliminary current-distance characteristics have been obtained.

Q-meter tests on the pancake-coil variable-impedance sensor have been concluded. Results indicate that the postulated skin depth-resistivity relation

is minimal. Information on sensitivity to diaphragm motion and diaphragm diameter along with response to misalignment and zero distance errors has also been obtained.

A pressure-temperature life test was conducted on a representative electrical terminal. The test was conducted at 1800°F for three consecutive 400 hour periods with pressurization values of 300, 600 and 1000 psia, respectively. No electrical or mechanical failure was noticed.

To achieve further flexibility in the Vacuum Test Facility, two test chambers have been fitted with individual ion type vacuum pumps. These chambers now can be operated independent of the facility itself.

Design configurations have been completed for potassium compatibility testing of the pressure capsules and the electrical terminal.

3.0 Pressure Capsule

Two FS-85 pressure capsules have been successfully fabricated. One of the capsules was fitted with a mechanical system to amplify the diaphragm motion; this system is described in the Second Quarterly Report (Reference 1). Both capsules were installed in the Vacuum Test Facility. It was decided to evaluate the diaphragm deflection measurement technique (Section 6.2) using the FS-85 capsule without the mechanical amplification system. Since data well within acceptable accuracy limits (± 20 micro-inches) were obtained from the un-amplified capsule, no tests were performed on the amplification system.

Two W-25 Re pressure capsules (ring/disc design) were fabricated. Both capsules developed weld failures during fabrication. One capsule failed in the Mo-50Re transition tube between the capsule and the pressurization system and the other developed a crack adjacent to the projection tip used for deflection measurements. The tip had been electron-beam welded into the bottom disc. Both capsules still had one good convolution each. The

capsule convolutions were separated by spark discharge machining and the two good convolutions were used to construct another capsule. This capsule was then installed in the test facility in place of the amplified FS-85 capsule. Work on another W-25Re capsule has been started using spark discharge machined discs.

A C-129Y capsule was successfully fabricated and installed in the test facility following completion of the pressure-deflection tests on the FS-85 capsule.

3.1 Test Results

To obtain as much deflection information as possible, it was decided to run pressure-deflection capsule tests using both 0.002 and 0.004 inch as maximum deflection parameters. The present status of the capsule experimental program may be summarized as follows.

FS-85:	0.002 inch max. deflection; to be done
	0.004 inch max. deflection; completed
W-25Re:	0.002 inch max. deflection; completed
	0.004 inch max. deflection; near completion
C-129Y:	0.002 inch max. deflection; near completion
	0.004 inch max. deflection; to be done

The test procedure being used includes the following steps.

1. Perform pressure-deflection calibration runs at room temperature, 500, 1000, 1200, 1400, 1600 and 1800°F.
2. Maintain full scale deflection and 1800°F for a 6 hour period. Measure the deflection. Unload the diaphragm and measure the zero pressure deflection. Repeat for 3 cycles.
3. Perform pressure-deflection calibration runs at 500, 1400 and 1800°F.

4. Apply overpressure to 200 percent maximum deflection (or until the diaphragm is close to the mechanical stop) at 1800⁰F for a 2 hour period. Measure the deflection every hour.
5. Perform pressure-deflection calibration runs at 500, 1400 and 1800⁰F.
6. Maintain full scale deflection and 1800⁰F for a 6 hour period.

Information from the test program may be grouped into three main areas of interest; pressure-deflection characteristics, full-scale deflection characteristics, and zero-pressure deflection characteristics. The effect of temperature on the reproducibility of these data must be determined along with any shifts exhibited with time (aging and permanent set effects). Using this information, efforts may be made to compensate for the temperature and time effects.

Figures 1-5 present the pressure-deflection data obtained from the initial calibration runs on the FS-85 capsule. At room temperature, 40 psia is required to obtain a deflection of 0.002 inch;

75 psia is required to obtain a deflection of 0.004 inch. At higher temperatures, the pressures required to obtain these deflections are steadily reduced. The relative straightness of the curves and the fact that zero closure (reproducibility of zero pressure deflection data between first and last readings in a particular test run) is obtained below 1800°F indicate that the elastic limit was not exceeded. The hysteresis effect exhibited by the 1800°F curves appears to be due to the maximum pressure used. The 1800°F recalibration runs, taken after the three-cycle sustained-pressure test, were run with a maximum pressure of 50 psia. These curves closely followed the increasing pressure portion of the initial 1800°F calibration but exhibited comparatively little hysteresis effect and good zero closure.

Pressure-deflection characteristics of the W-25Re capsule are shown in Figures 6-12. As with the FS-85 capsule, the deflection obtained for maximum test pressure increases with temperature, as does the hysteresis effect. However, zero closure is obtained at all temperatures. For equivalent pressures, the W-25 Re capsule exhibits about one-half the deflection of the FS-85 unit.

The 500°F pressure-deflection characteristic (Figure 7) was established by disregarding two data points (30 and 45 psia) which were apparently in error. There was no evident reason for these points to deviate from the characteristic. It does not appear that the errors signify a fault in the capsule since deflection data taken after the questionable points yield reasonable and expected results.

The W-25Re maximum deflection readings (60 psia, 1800°F) were found to vary between 0.00185 and 0.00223 inch through the test. However, after the initial calibration reading (0.00223 inch), the spread was from 0.00185 to 0.00202 inch. This suggests a possible permanent set effect introduced by the initial calibration runs.

Figure 13 presents data on the full scale deflections obtained on the FS-85 (at 87 psia) and the W-25Re (at 60 psia) capsules as functions of the operating temperature. Both capsules employed diaphragms of 0.52 inch radius.

The zero pressure deflections on the W-25Re capsule remained fairly constant throughout the initial calibration runs. However, during the three-cycle sustained-pressure test, the capsule

appeared to take a set of about 0.0015 inch. The zero pressure deflection then remained fairly constant, at this new level, until the end of the test.

4.0 Deflection-Electrical Signal

During the report period, emphasis was on experimental evaluation of the thermionic diode and variable impedance sensors. An improved thermionic device was designed and built, and preliminary current-distance characteristics were obtained which verify feasibility of the thermionic approach. Q-meter testing was concluded on the pancake-coil variable-impedance sensor.

The criteria used for evaluation of the transduction system involve signal level and deflection range. The deflection should be as small as possible, consistent with usable output, to minimize the stress levels in the diaphragm. An output level as high as 64 milliamperes for a deflection of 0.002 inch has been

obtained from the thermionic diode. For the variable impedance device, the maximum inductance change observed for a diaphragm travel of 0.002 inch was less than 0.3 microhenry. It is unlikely that the impedance bridge output under these conditions could match the output performance of the thermionic diode. In addition, the variable impedance device is a high frequency system with the attendant transmission line considerations as opposed to the relatively straight forward low voltage dc thermionic system. Although a rigorous and exhaustive comparison has not been made, it appears that future work on the transduction system should be limited to the thermionic sensor.

4.1 Thermionic Diode Sensor

The thermionic device described in the Second Quarterly Report (Reference 1) was assembled and installed in the Vacuum Test Facility. A double W-25Re heater was used to improve heater temperature-strength characteristics. Additional anchor points and ceramic insulators were included to improve mechanical stability and prevent any electrical shorting problems. However, during the emitter activation procedure, gas-discharge was observed between the emitter and the movable collector. This appeared to be due to accumulation of out-gassing products in the interelectrode space. The inclusion of more evacuation holes in the collector was indicated. Upon disassembly of the unit, a deposit of copper was observed on the movable collector. It appeared that the collector was running relatively cool and acting as a condensing surface for copper evaporating out of the brazing material used to join the support tube to the conical shaped adapter of the device.

In view of these difficulties, a redesign was undertaken incorporating the following changes:

1. The use of brazing materials was eliminated.
2. The dual emitter assembly was modified to accommodate a larger heater. A commercial, ceramic-insulated, double spiral wound heater was used.
3. The emitter holding plate was webbed to minimize thermal conduction losses to the surrounding support structure.
4. The collectors were webbed to allow effective evacuation of the interelectrode spaces.
5. A ceramic coupling was used close to the movable collector and connecting it to the push rod. This minimizes thermal conduction losses from the collector and effectively raises its operating temperature.
6. An open type construction was used to facilitate optical pyrometer readings on the emitters.

Figure 14 presents an assembly view of the dual diode and Figure 15 shows the device mounted and ready for installation in the Vacuum Test Facility. The reference collector is mechanically fixed 0.006

inch from its emitter. The active collector-emitter distance is adjustable between 0.004 and 0.006 inch by means of the micrometer assembly mounted on the vacuum chamber flange. The mechanism is such that for one revolution of the micrometer (250 gradations), the active collector is displaced 0.002 inch.

4.1.1 Test Results

The thermionic test device was installed in the Vacuum Test Facility and the ambient temperature raised to 1800°F. After initial outgassing, the heater was energized and emitter activation was accomplished. Heater input parameters resulting in 2100°F emitter operation were 12.5 volts, 1.15 amperes, 60 cps. The circuit of Figure 16A was used to obtain the current-distance characteristics of Figure 17. The test procedure employed is as follows:

1. The voltage V is set at some arbitrary value. For the tests, values for V of 10, 12, 16 and 20 volts were used.
2. The emitter - active collector distance is adjusted through the micrometer until the active collector current i_a matches the reference collector current i_r . The sum $(i_a + i_r)$ is noted.
3. The emitter - active collector distance is then decreased 0.0002 inch (25 micrometer graduations). This causes a change in i_a ,

and in $(i_a + i_r)$. The voltage V is then adjusted so that the sum $(i_a + i_r)$ is restored to the value obtained in (2) above. Under this condition, the difference current $(i_a - i_r)$ is calculated and plotted in Figure 17.

It should be noted that the milliammeters used were accurate to ± 1 ma (± 1 percent full scale). Since the current difference is being calculated, there exists a "zone of error" of ± 2 ma surrounding each curve of Figure 17. It can be seen that the data points lie within the "zone of error" associated with their respective curves. To increase the accuracy of future measurements and further demonstrate the feasibility of this approach, precision resistors (1.000 ohm) and a highly accurate digital voltmeter (capable of reading to 0.1 mv with an accuracy of ± 0.5 percent) will be used to obtain direct readings of i_a , i_r , $(i_a + i_r)$ and $i_a - i_r$. It is expected that this will minimize,

if not eliminate, the "zone of error". The circuit to be used is shown in Figure 16B. The voltmeter connections and the corresponding parameters read by the voltmeter are:

<u>Voltmeter Connections</u>	<u>Reading</u>
1-2	i_a
1-3	i_r
4-5	$(i_a + i_r)$
3-2	$(i_a - i_r)$
1-5	V

The voltmeter connections will be changed through a two-pole, five-position rotary switch.

4.2 Variable Impedance Sensor

Q-meter testing was concluded on the pancake-coil variable-impedance sensor. In addition to obtaining the inductance-distance characteristics, efforts were made to determine:

1. System sensitivity to small changes in coil-diaphragm distance,
2. System error introduced by coil-diaphragm angular misalignment,
3. System response to changes in diaphragm diameter and
4. System error introduced by coil-diaphragm zero spacing error.

4.2.1 Test Results

Typical inductance-distance curves using diaphragms of various resistivities and the pancake-coil described in the Second Quarterly Report (Reference 1) are shown in Figures 18 through 20. Coil - diaphragm distances of up to 0.070 inch are shown. For greater distances, the curves tend to flatten out and approach an inductance value of 4 microhenries at 0.2 inch, independent of diaphragm material. It appears that the skin depth change with resistivity, upon which the analytical model of the variable impedance device is based, is a minimal effect. There is no definite displacement of the curves with increasing resistivity. To ascertain whether the results might reflect instrumentation and set-up errors, known spacing and alignment errors were introduced in later tests with the following results.

Pancake-coil response to changes of 0.0001 inch (5 percent of an assumed total diaphragm travel of 0.002 inch) in coil - diaphragm

distance was measured. Tests run at distances of 0.010, 0.030, and 0.060 inch showed a change of less than 1 percent in the measured inductance. This percentage change was independent of diaphragm material, thickness and diameter. It therefore appears that the system is relatively insensitive to small changes in spacing.

Spot checks made on the effect of coil - diaphragm angular misalignment showed inductance changes of 2-3 percent for an alignment error of 1 degree. However, a 1 degree error is easily noted by visual observation and the normal experimental run is made with errors well below this 1 degree value. It therefore appears that misalignment is not a cause of the inconclusive results of Figures 18 through 20.

Tests conducted using 1, 1-1/2 and 2 inch diameter diaphragms of copper, cupronickel, monel and K-monel failed to yield any consistent inductance change with diaphragm diameter. These materials represent a range of resistivities

corresponding to the values expected in operating a refractory alloy up to 1800°F.

Using a dial indicator to ascertain the coil-diaphragm zero spacing, it was possible to reproduce the zero spacing results within 5-15 percent. It should be remembered that although the actual zero spacing may be determined to better than 0.001 inch with the dial indicator, the Q-meter is operating with the lowest possible Q-value for the pancake-coil. This makes a relatively large operator error quite possible. It is felt that this difficulty in reading the Q-meter at very small coil - diaphragm distances is the most likely cause of the inconclusive results concerning the reproducibility of the induction at zero spacing.

5.0 Electrical Terminal

One of a group of terminals ordered for inclusion in the test program has been subjected to a series of life tests. The test configuration is shown in Figure 21. Three consecutive tests were performed with the following parameters:

400 hours, 1800°F, 300 psia pressurization.

400 hours, 1800°F, 600 psia pressurization.

400 hours, 1800°F, 1000 psia pressurization.

No electrical breakdown or mechanical failure (leakage) was observed. Ohmmeter readings taken between the electrical feed-through terminal and ground remained fairly constant at 9-11 kilo-ohms through the 300 and 600 psia tests. A steady increase in resistance from 10 to 25 kilo-ohms was observed during the 1000 psia test. The cold resistance value is 80 kilo-ohms. Because of the relative scarcity of terminals, the life test terminal will not be dissected for examination immediately but will be used for possible future testing (including an internal pressurization test).

It is expected that another terminal will be subjected to the life test procedure to corroborate the results.

6.0 Vacuum Test Facility

Test experience on the facility indicates the desirability of being able to operate individual test chambers independent of the facility itself. This need is exemplified by the emitter activation of the thermionic device. It is necessary to perform activation on a continuous basis at a pressure below 10^{-7} Torr. This vacuum is impossible to maintain when a test is started in one of the other chambers. The initial outgassing raises the pressure to the point where it was necessary to shut down the thermionic test. To remedy this difficulty, individual ion type pumps (5 liters per second) have been fitted to the two end test chambers. An installation is shown in Figure 22. It is now possible to operate these chambers valved off from the facility manifold. Thermionic device testing is being performed in one of these chambers.

6.1 Liquid Potassium Compatibility

Design configurations have been completed for potassium compatibility testing of the pressure capsules and the electrical terminals. Figures 23 through 25 show the designs. To expedite fabrication of the test devices, only one convolution will be used in the pressure capsules and there will be no containment housing around the capsules. There will be a yoke arrangement to act as a mechanical stop against excessive displacement and subsequent failure of the diaphragm disc.

Figure 23 shows the design for the columbium and tantalum alloy capsules (FS-85, C-129Y, T-222). The two-piece yoke and potassium containment tube are made of FS-85 alloy.

Figure 24 shows the design related to the W-25Re alloy capsule (spark discharge machined discs) and utilizes Mo-50Re tubing as a transition between the W-25Re capsule and the molybdenum yoke and TZM potassium containment tube.

A Mo-50Re ring is also used as a weld insert between the thermocouple well and the potassium containment tube.

Figure 25 shows the electrical terminal test configuration. It is intended to use a fixture capable of accepting four terminals for test. Since the electron-beam welding of the terminal cap is done in a vacuum of about 10^{-4} Torr, zirconium has been inserted in the terminal assembly to act as an oxygen getter. Prior to the actual preparation of the compatibility devices, mock-ups are being prepared for dummy runs to establish procedures for potassium charging and capsule closure (electron-beam welding the thermocouple well to the containment tube).

Calculations indicate that each device will be charged with 0.23 cubic inch of liquid potassium at room temperature. When the temperature of the two-phase interface is raised to 2300°F to establish a vapor pressure of 300 psia, the

level will rise. Due to the fact that the internal volumes of the respective devices below the freezing level of the potassium charge are not exactly equal, the levels will rise about 1/2 and 3/4 inch for the two devices. In any event, during operation, the thermocouple will be sufficiently above the liquid-gas interface to ensure proper measurements.

The test parts themselves will be maintained at 1800°F and monitored by pyrometry through the test chamber viewing window.

Design work is currently in progress to modify the interior of the test chamber to accept the auxiliary heater and heat shields needed to raise the interface temperature.

6.2 Diaphragm Deflection Measurement

During the report period, work on deflection measurement was concentrated in two areas. One involved techniques for marking the capsule parts; the other concerned procedures for obtaining and processing the photos and extracting the data.

Two methods of marking the capsules were tried; the use of diamond indentors from hardness testing equipment and surface treating with a commercial abrasive unit (results in a cratered surface with high spots that reflect illumination). Both techniques provide more distinct and recognizable characteristics than the scribed lines used previously. The lack of adequate space on the capsule dictated the use of the abrasive surface-treatment and this method has been used exclusively.

Green light illumination is directed through one ocular of a binocular microscope (40X magnification) into the test chamber. The camera is attached to the other ocular system. The final readings are taken from the developed plates on

a shadowgraph instrument capable of an accuracy of 0.0001 inch. Since the camera system operates at 40X magnification, this instrument accuracy corresponds to a marking distance of 2.5 micro-inches. A typical plate is shown in Figure 26. The plates are set in the shadowgraph so that readings of the reference marking distance are repeated from plate to plate. From this base, measurements are taken on the deflection marking distance.

Experience has shown that the deflection data obtained between two capsule marking points can be read on the shadowgraph with a spread of less than 0.001 inch (± 12.5 microinches actual distance) between the high and low readings in a set of ten. This is well below the original desired accuracy of ± 20 microinches. Statistical treatment of the data, which gives less weight to readings at the extremes, would result in better accuracy. Since data obtained from any five readings in the set could not be more

inaccurate than that obtained from ten, it was decided to lower the number of readings used to obtain an average from ten to five. This has considerably speeded up the data gathering process.

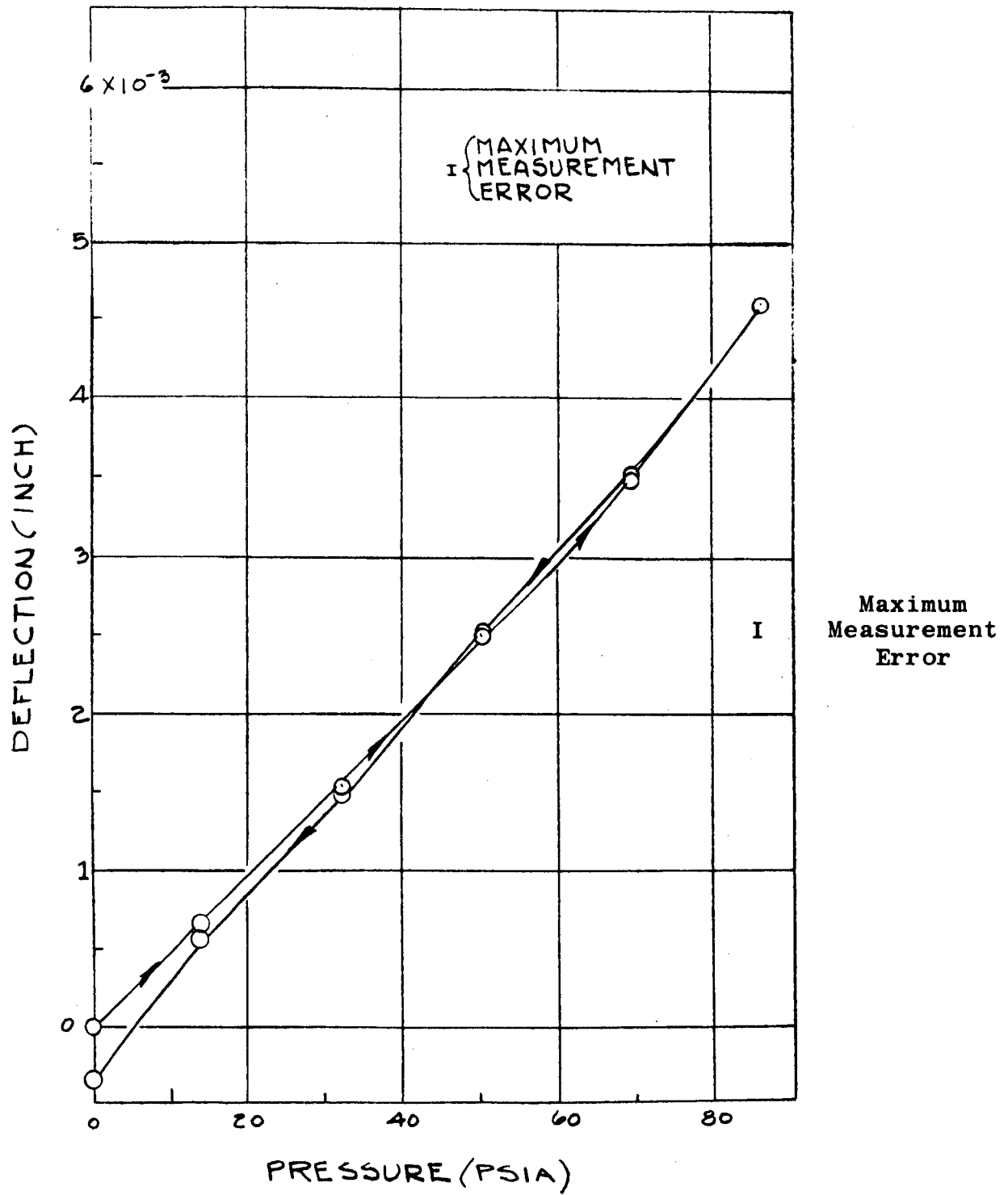


Figure 1

FS-85 Pressure-Deflection; Room Temperature

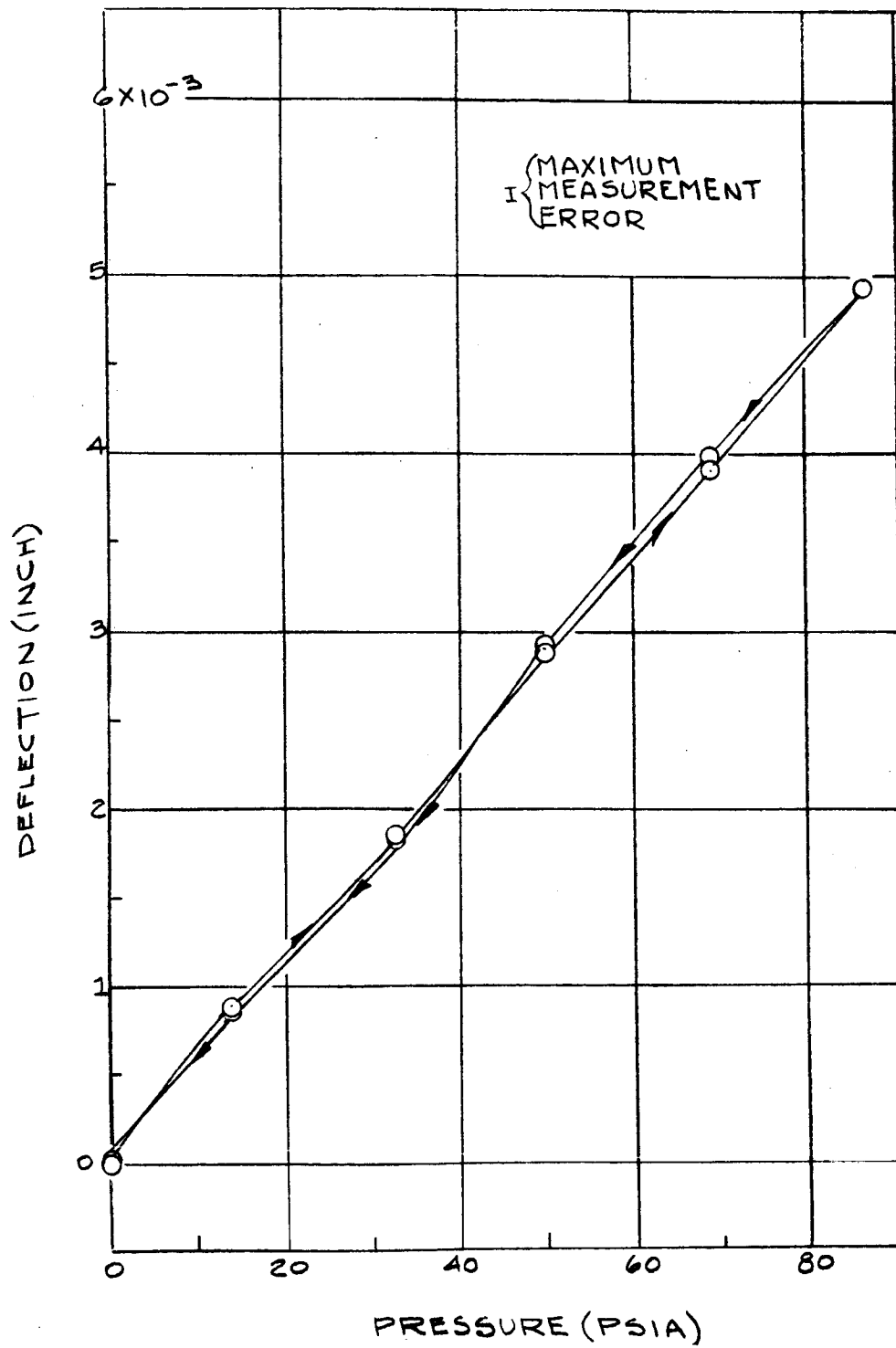


Figure 2

FS-85 Pressure-Deflection; 500°F

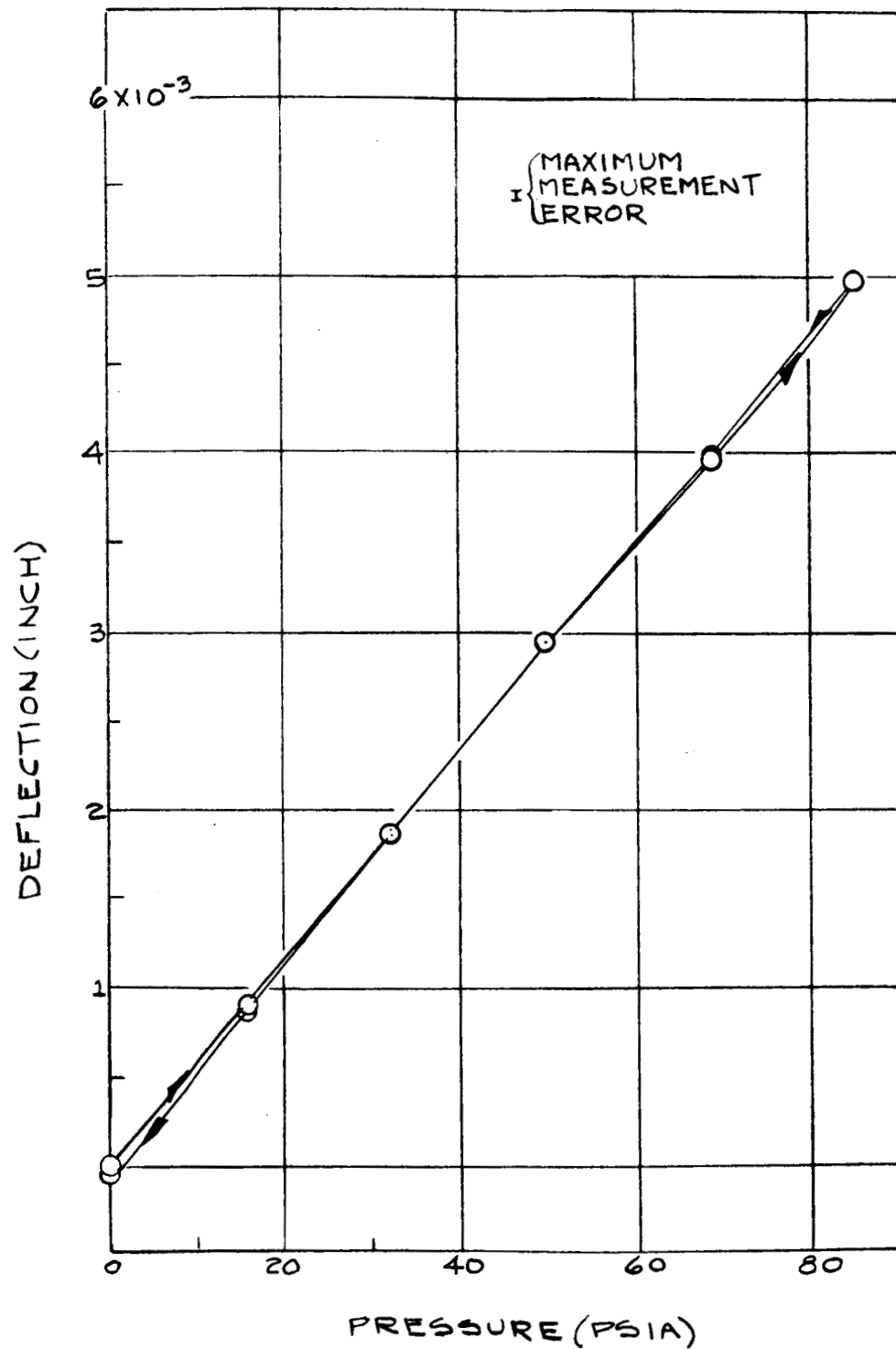


Figure 3

FS-85 Pressure-Deflection; 1000°F

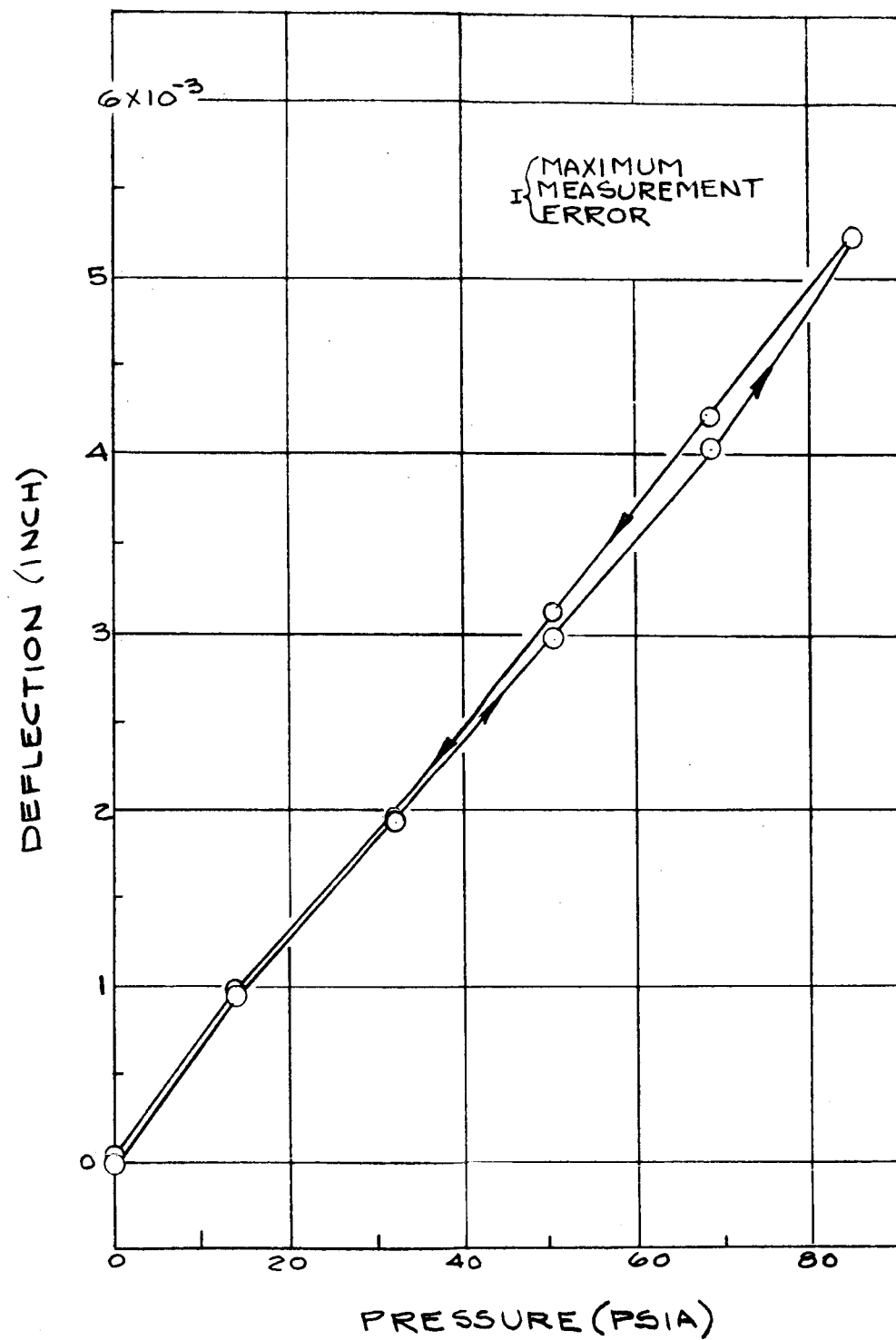


Figure 4

FS-85 Pressure-Deflection; 1400°F

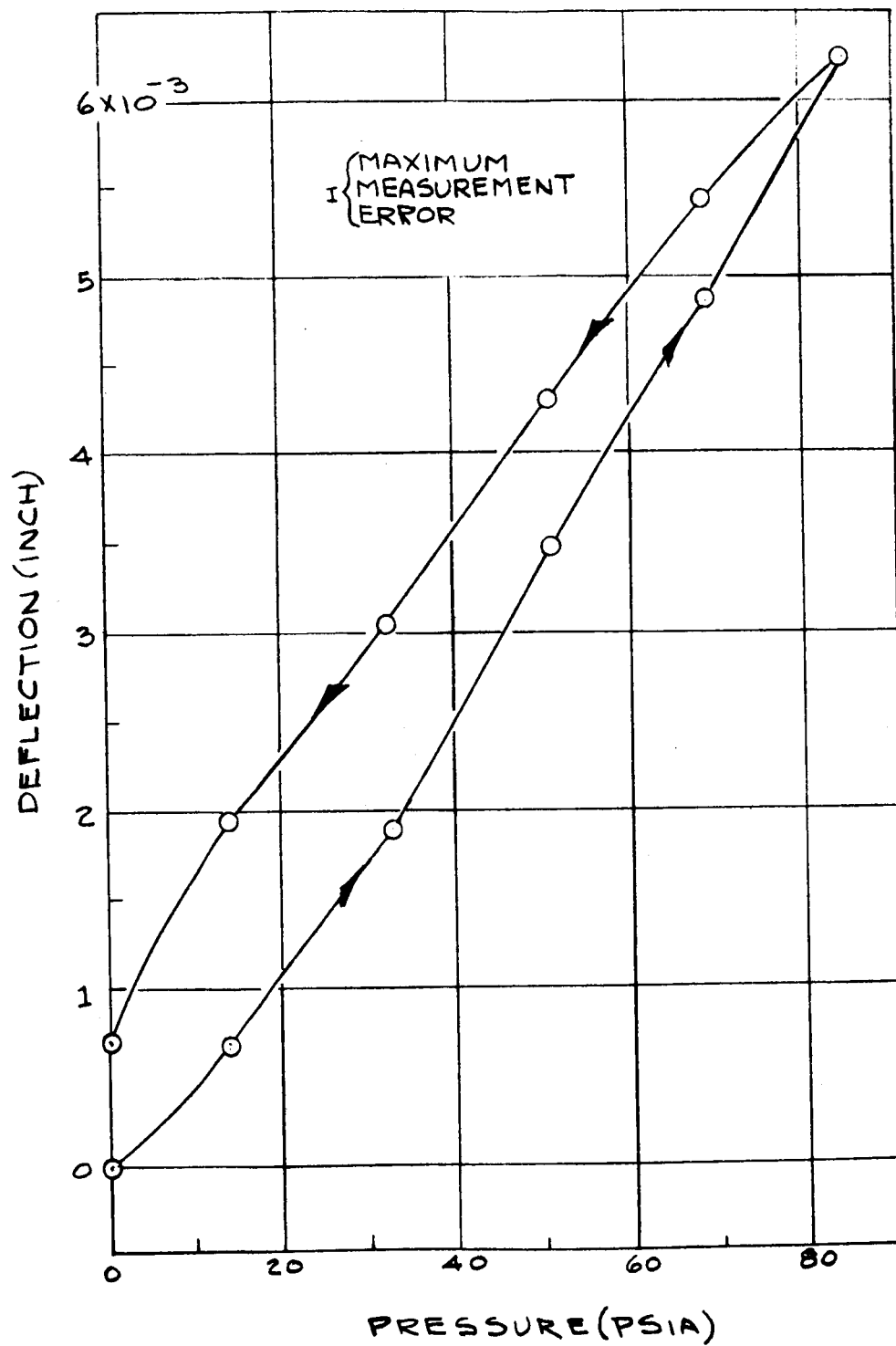


Figure 5

FS-85 Pressure-Deflection; 1800°F

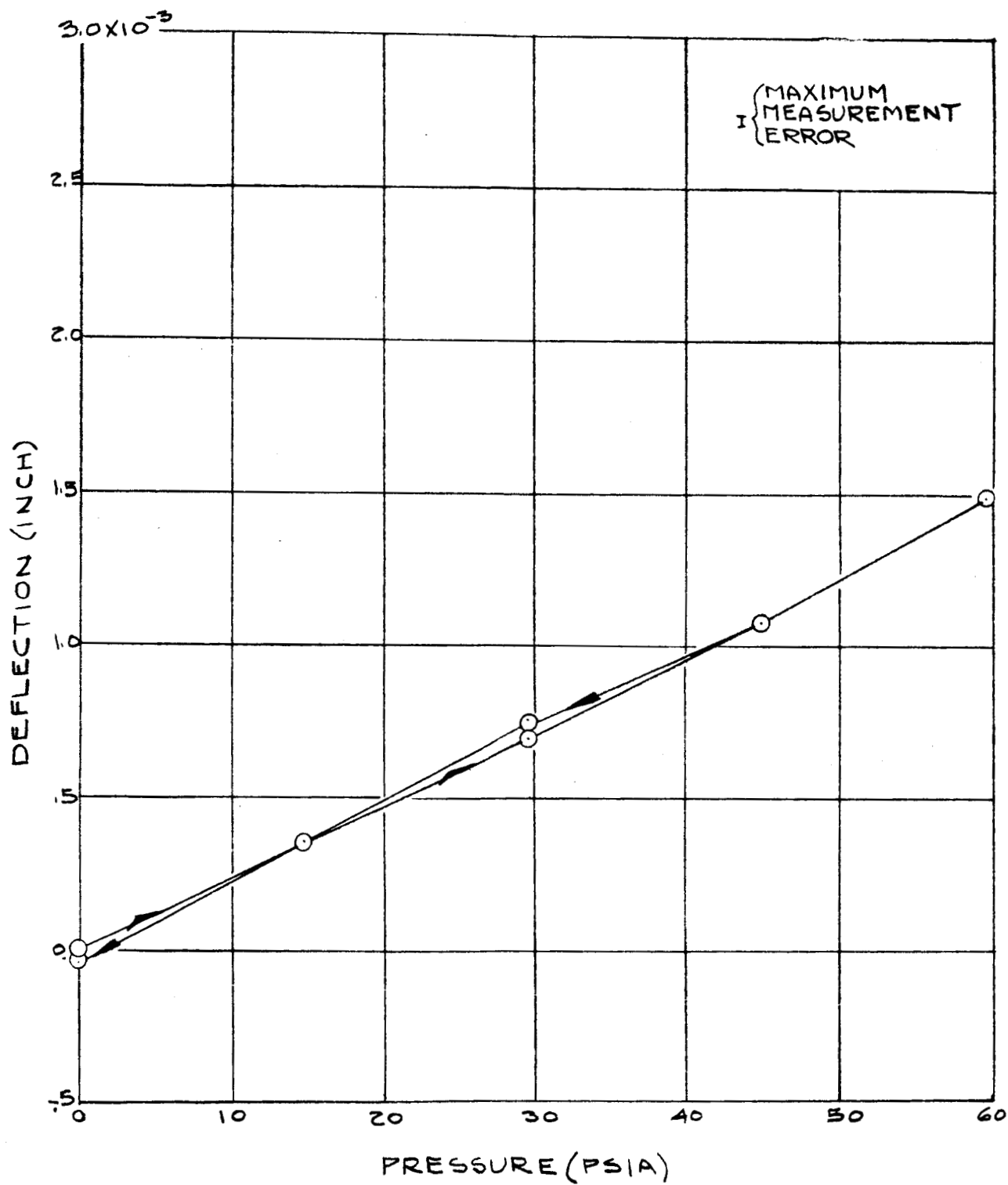


Figure 6

W-25Re Pressure-Deflection; Room Temperature

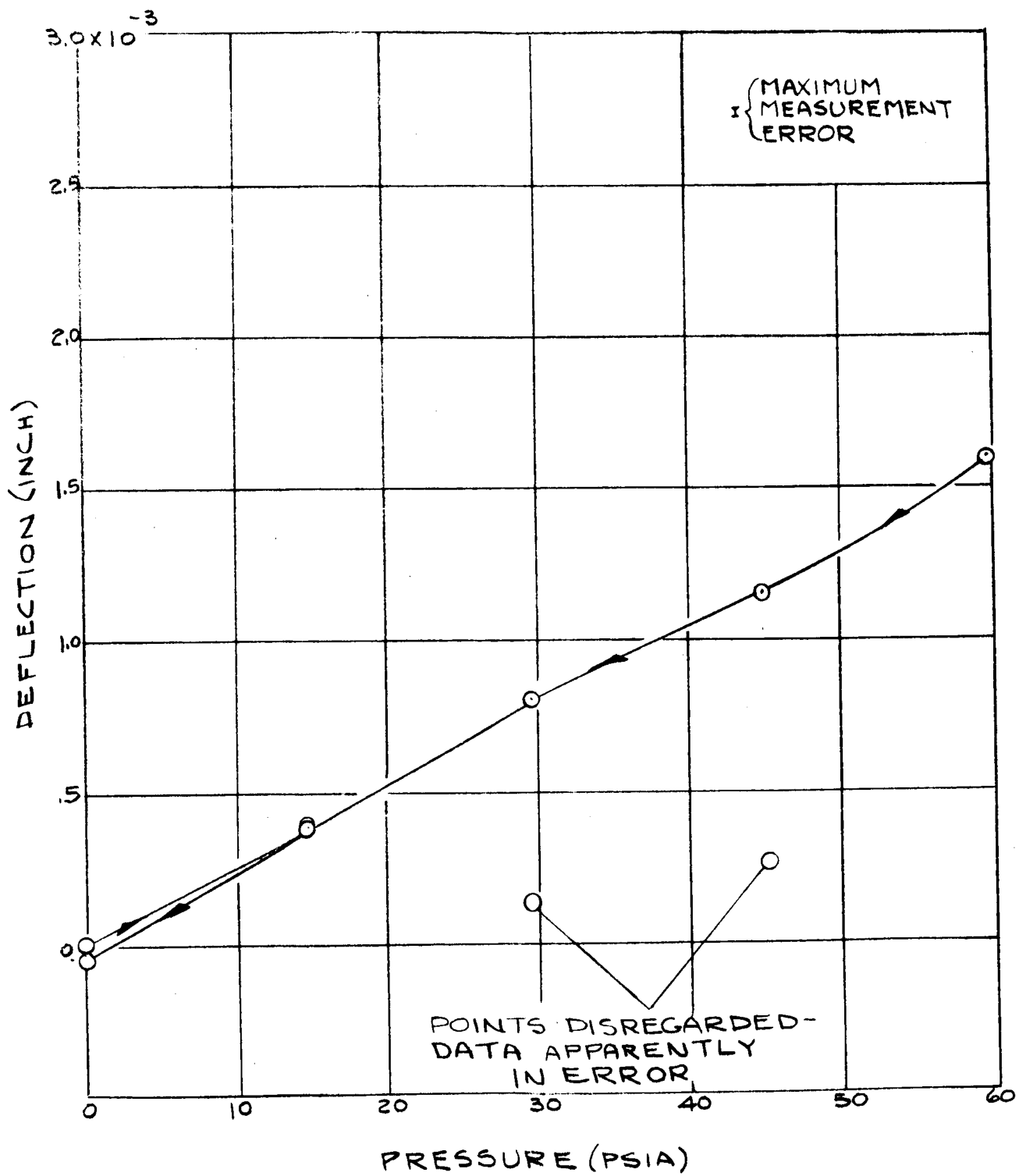


Figure 7

W-25Re Pressure-Deflection; 500°F

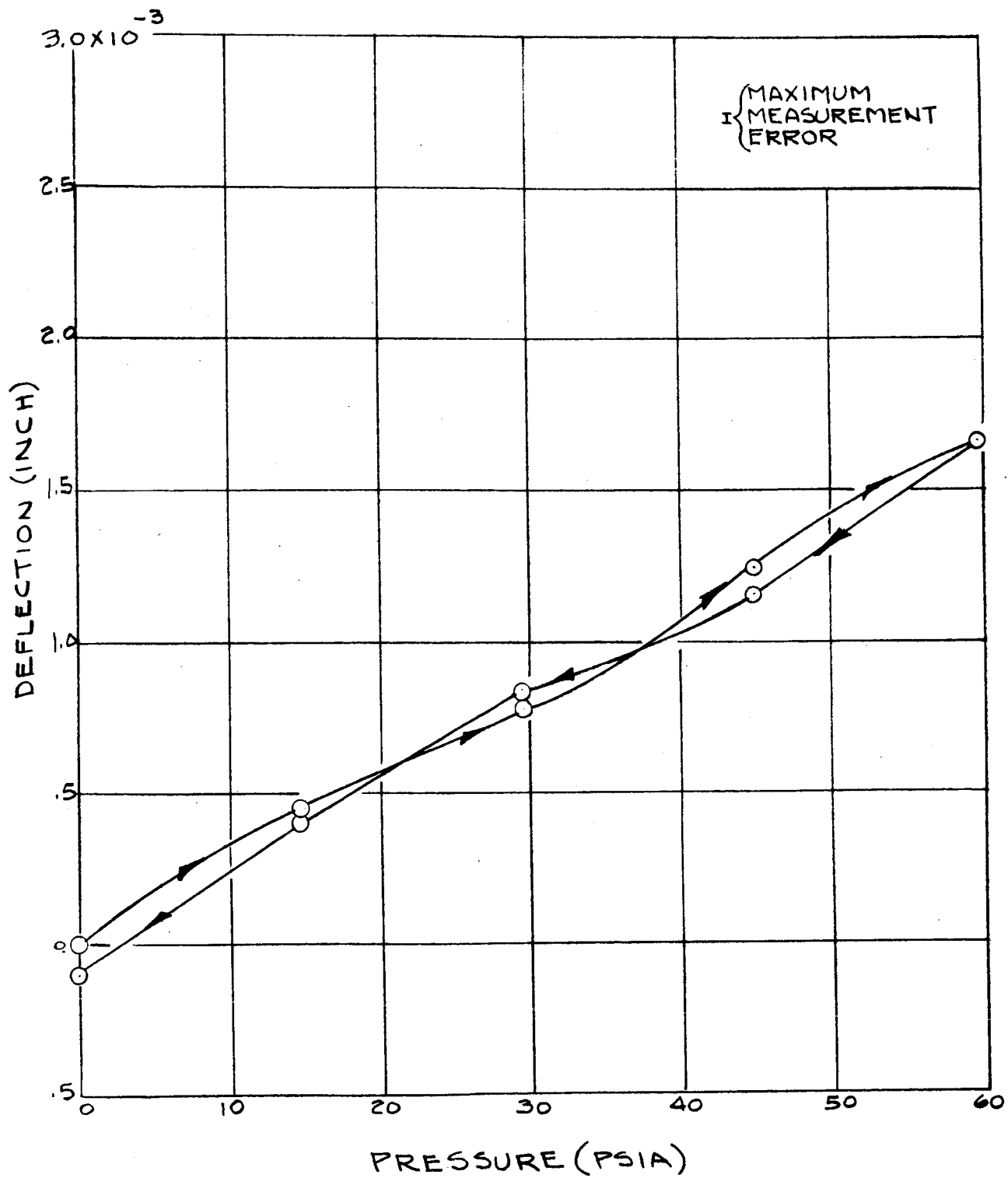


Figure 8

W-25Re Pressure-Deflection; 1000°F

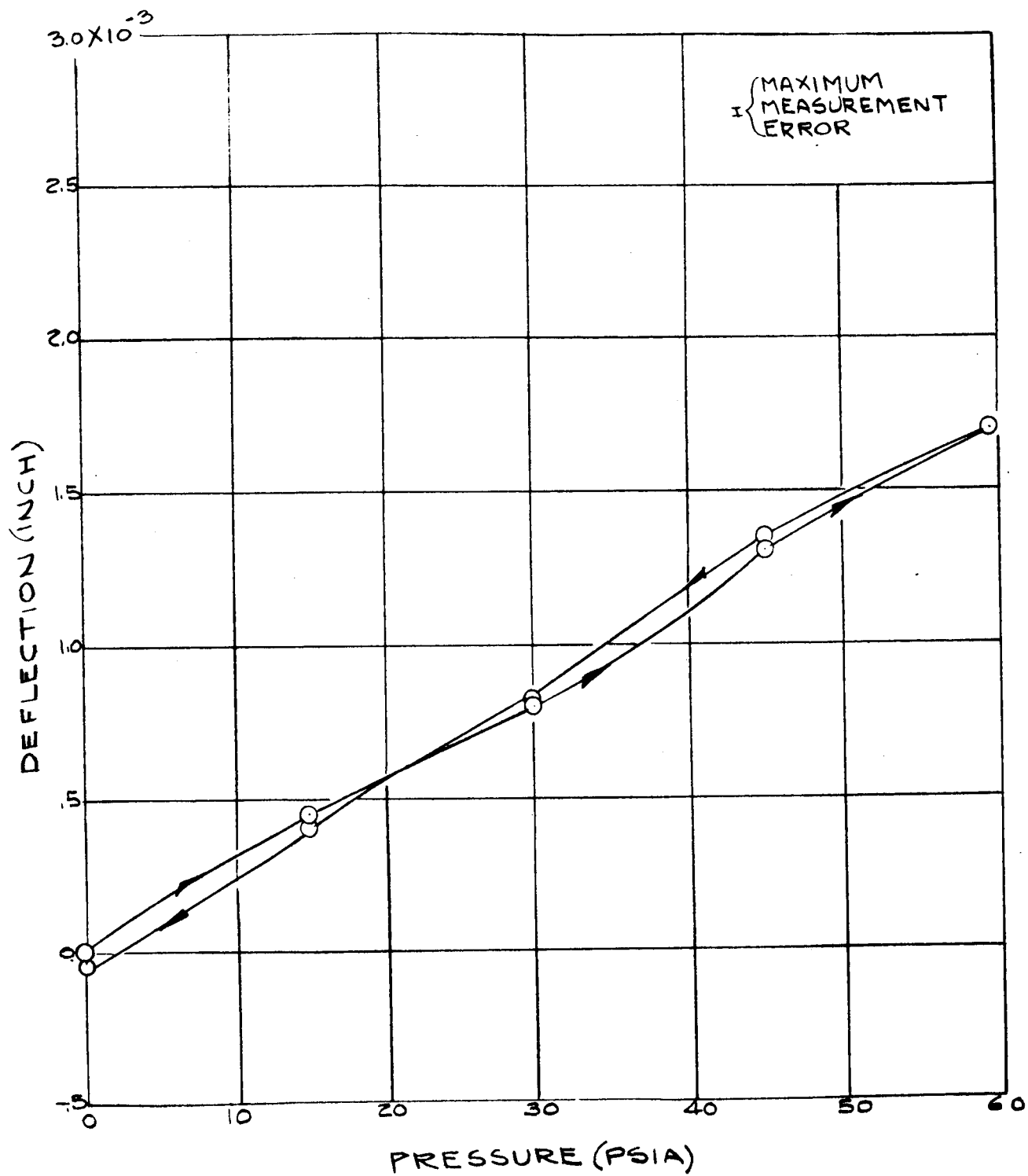


Figure 9

W-25Re Pressure-Deflection; 1200°F

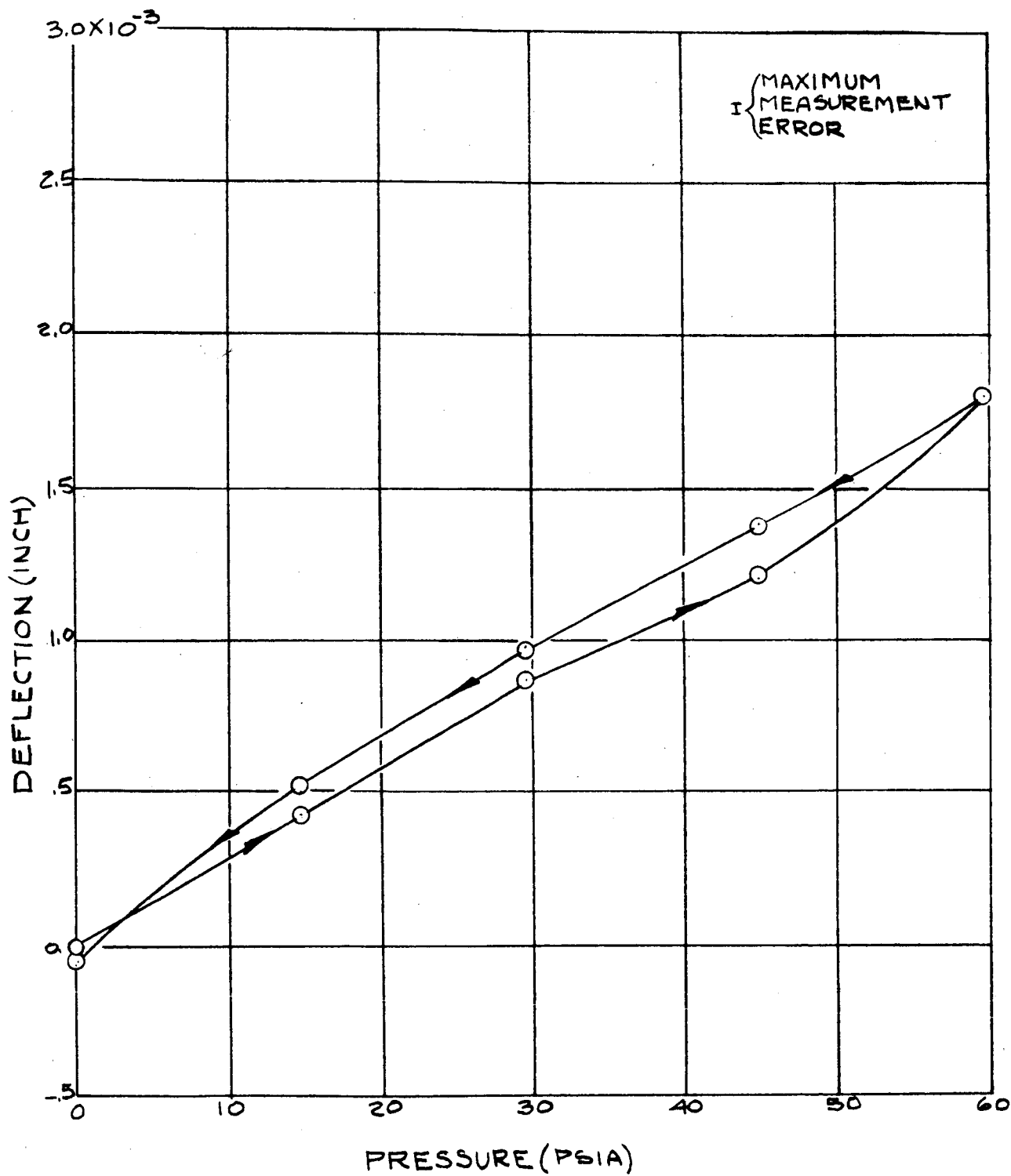


Figure 10

W-25Re Pressure-Deflection; 1400°F

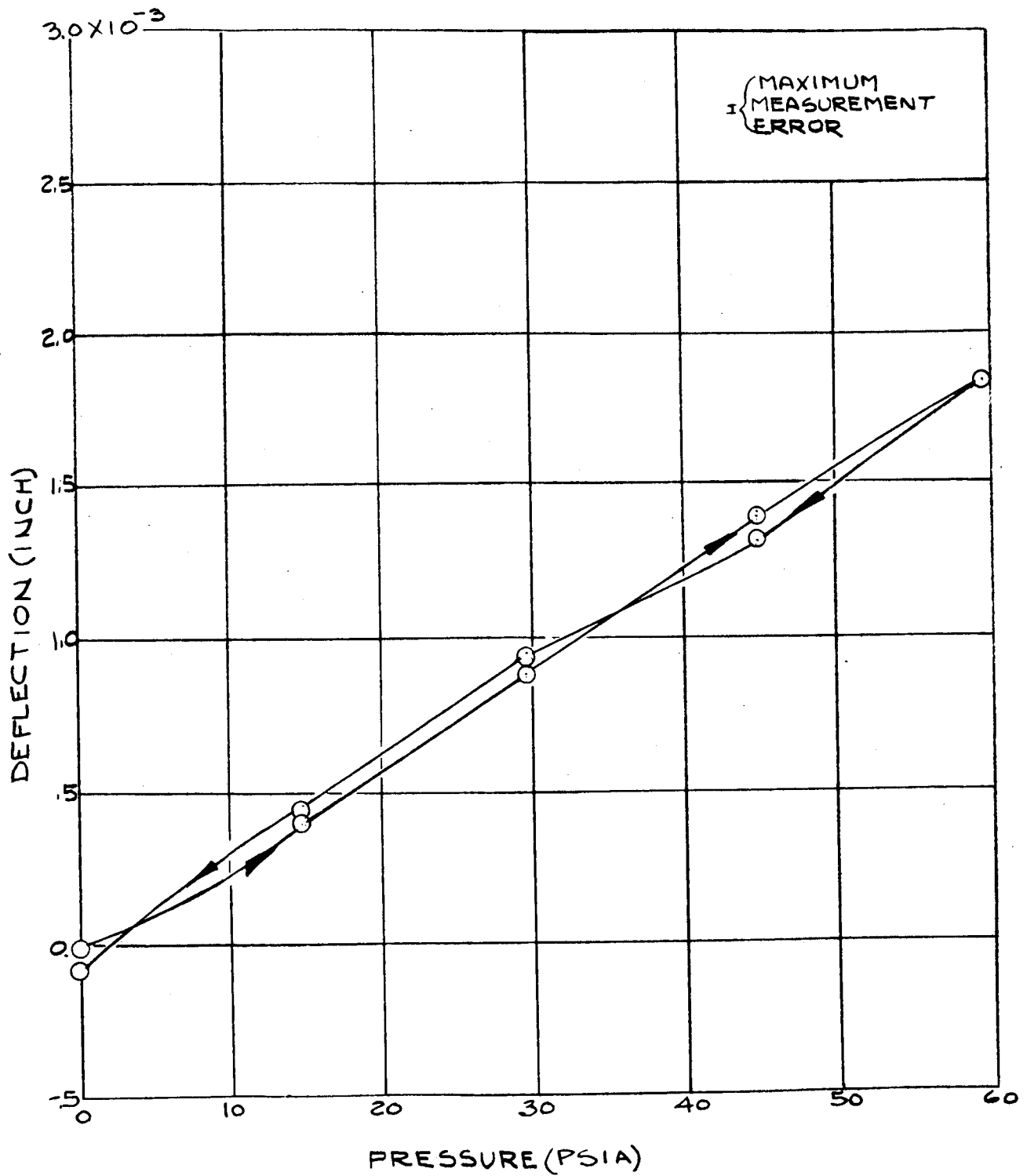


Figure 11

W-25Re Pressure-Deflection; 1600°F

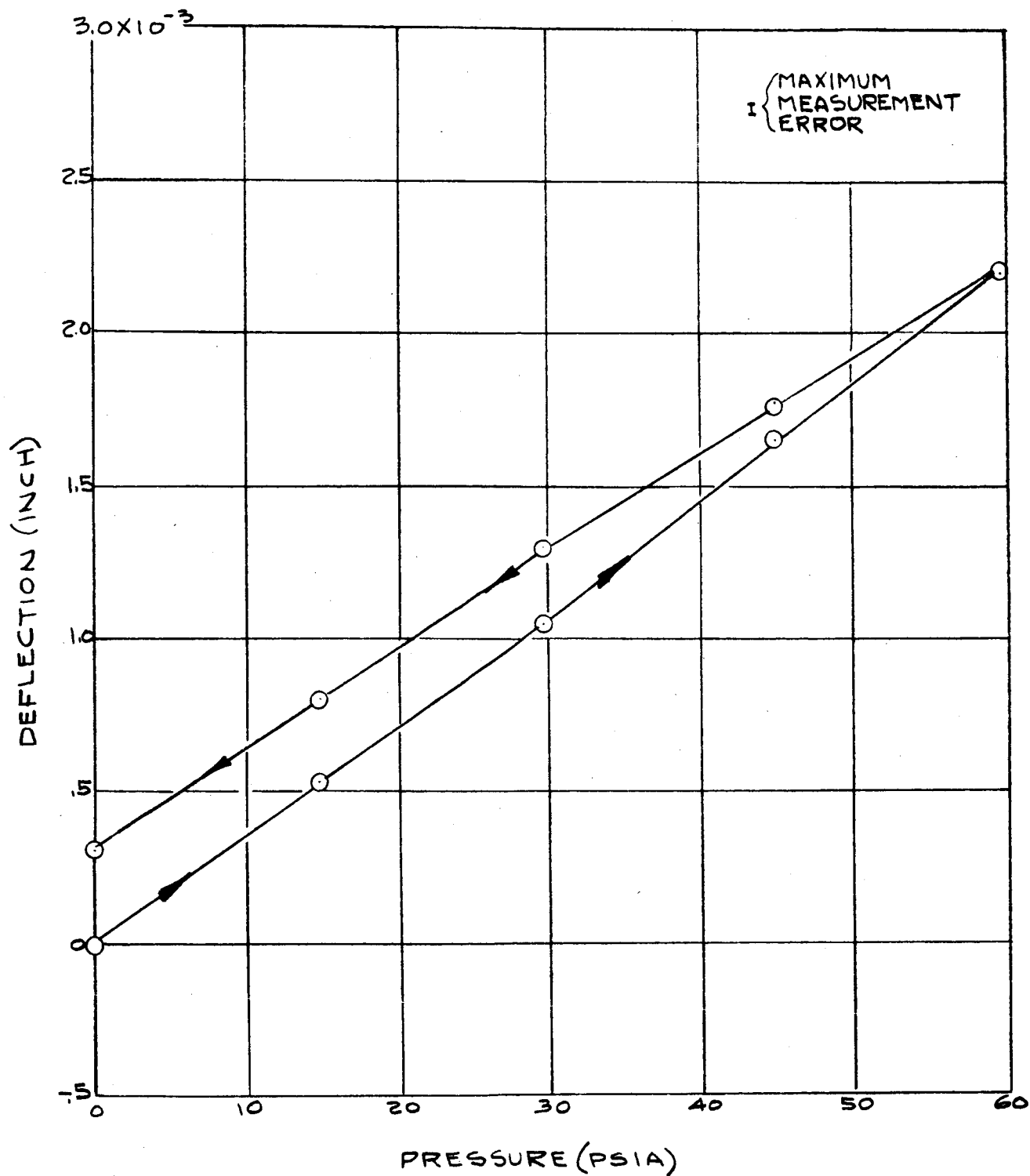


Figure 12

W-25Re Pressure-Deflection; 1800°F

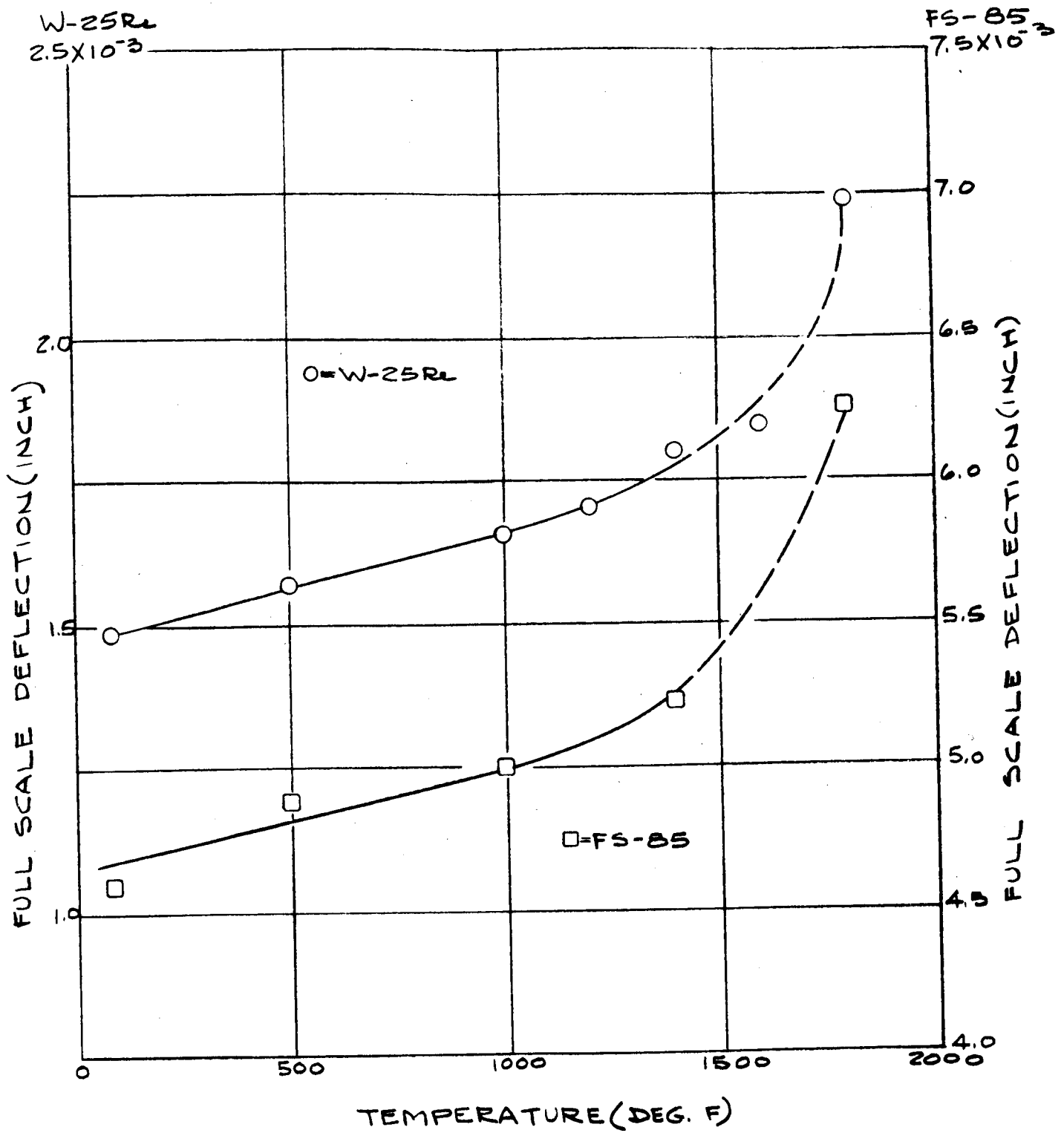


Figure 13

Full Scale Deflection-Temperature Characteristics

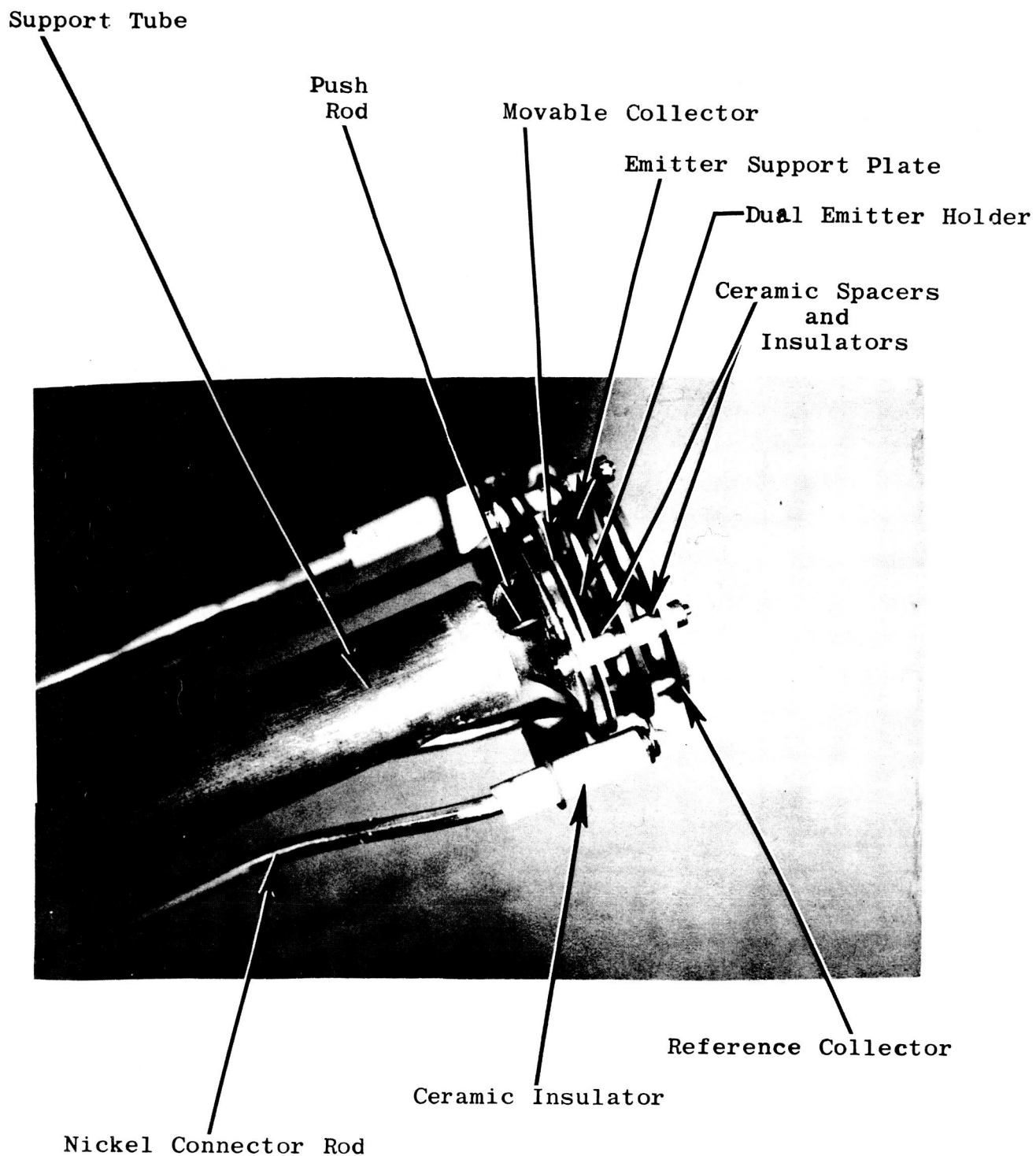


Figure 14
Dual Emitter Test Device

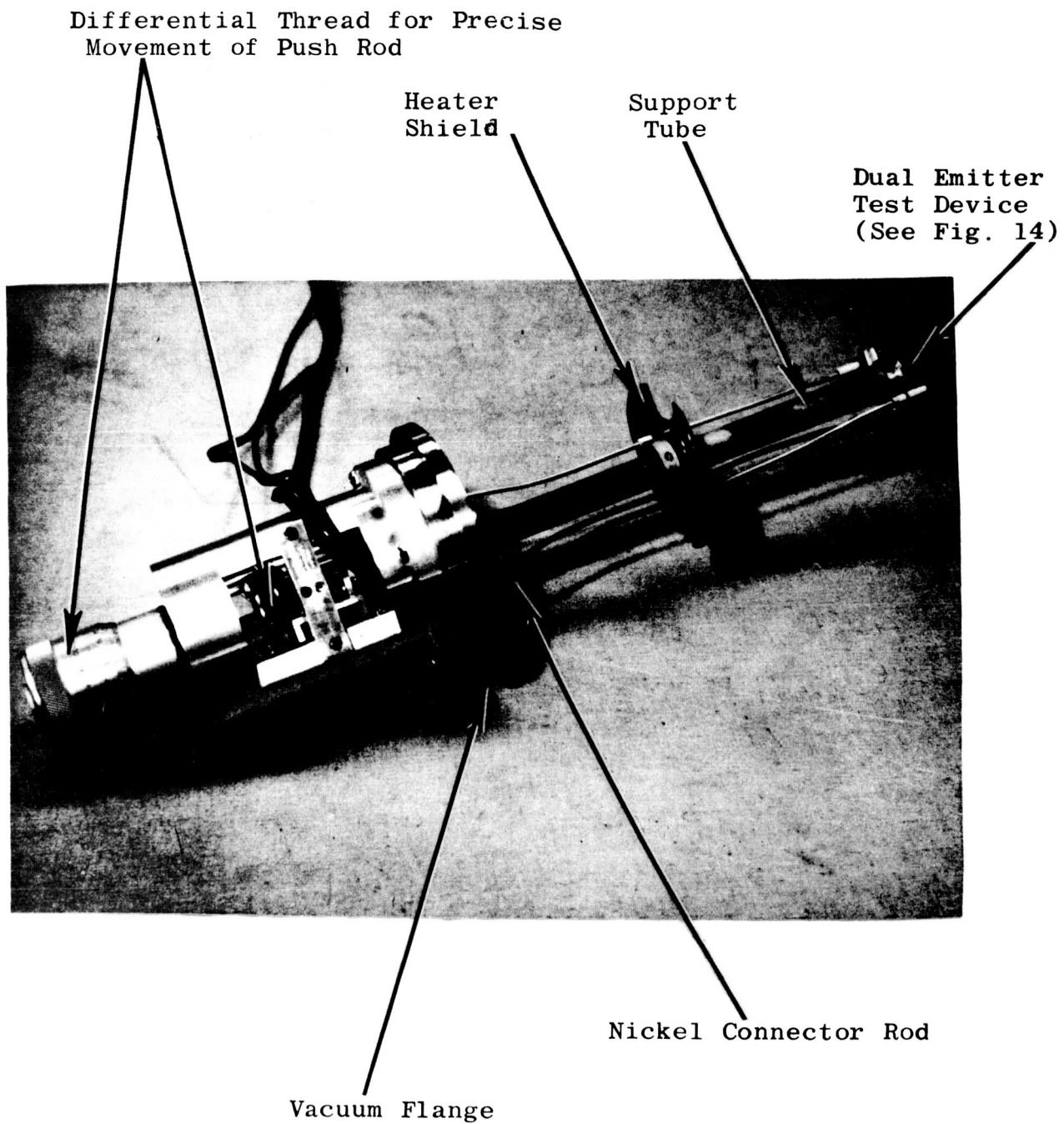


Figure 15

Dual Emitter Test Device; Vacuum Chamber Installation

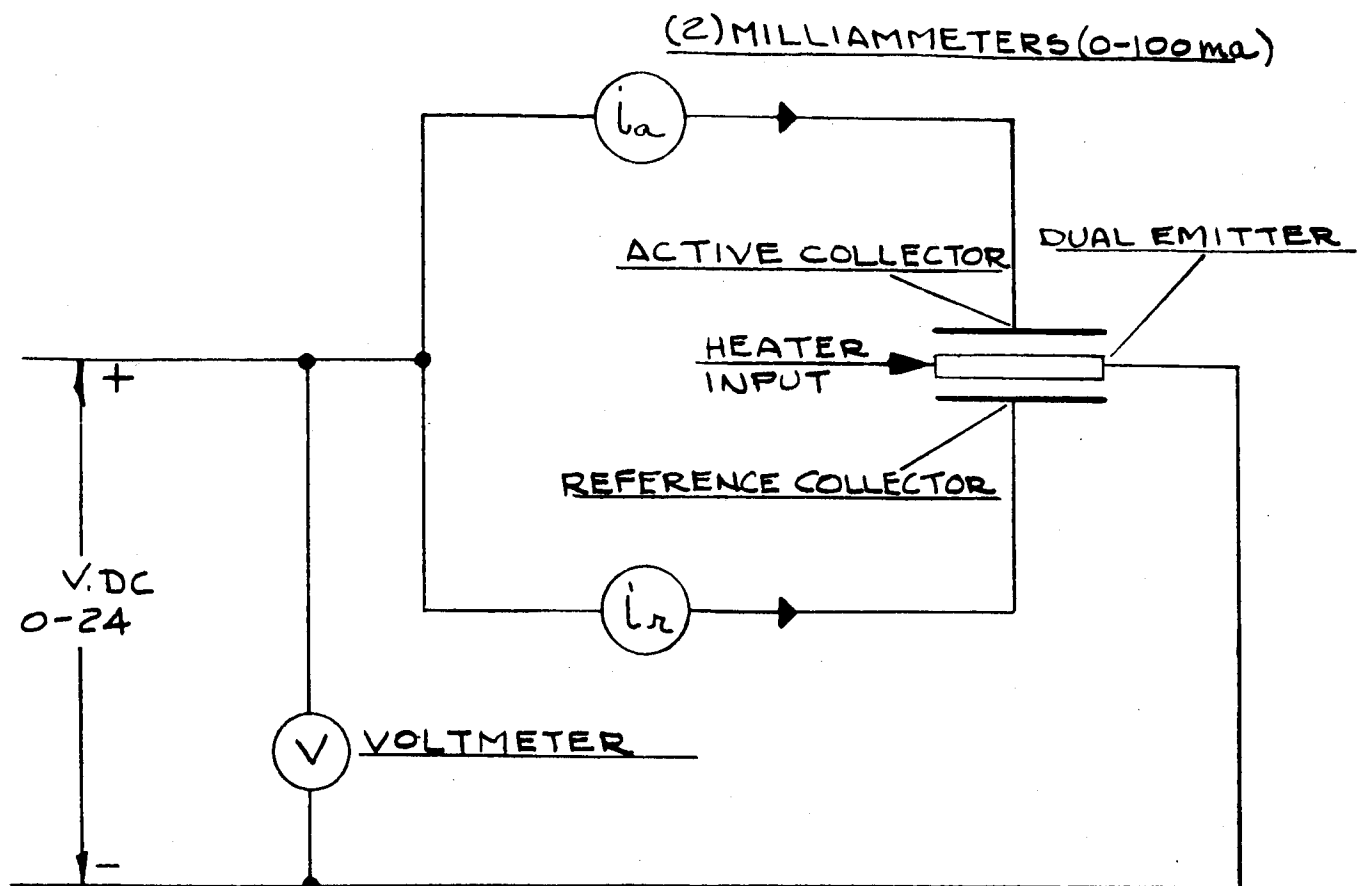
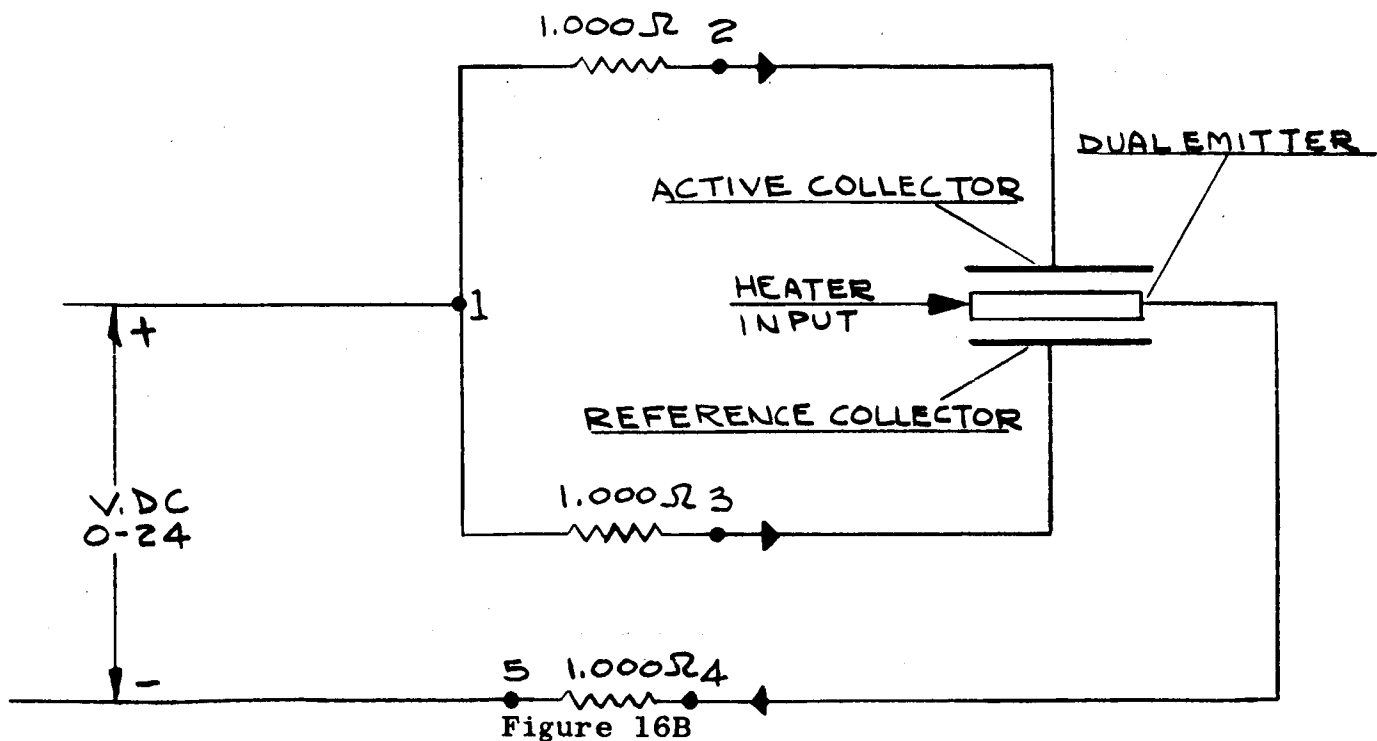


Figure 16A

Thermionic Test Circuitry



Thermionic Test Circuitry

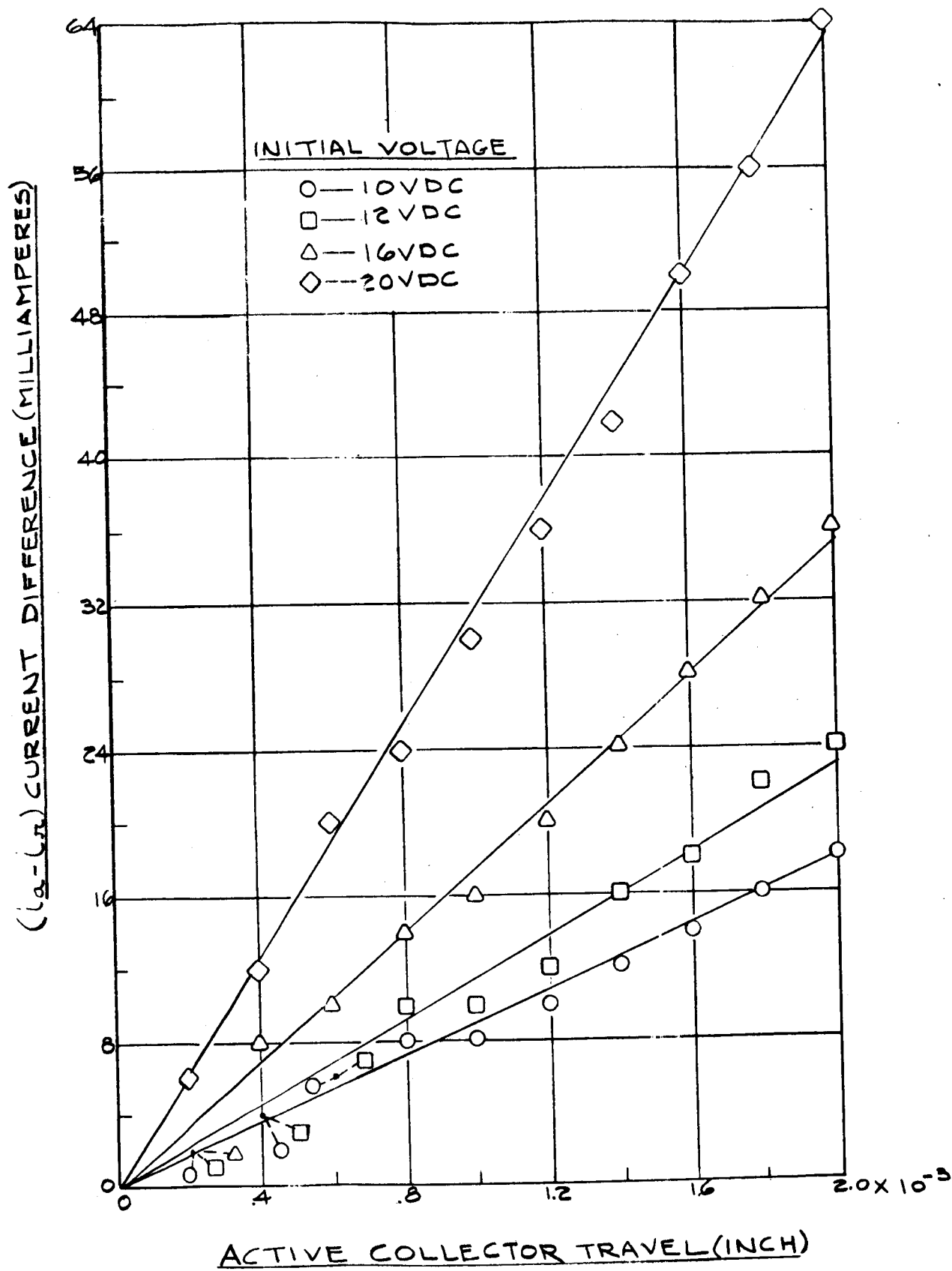


Figure 17

Current-Distance Characteristics; Thermionic Sensor at 1800°F

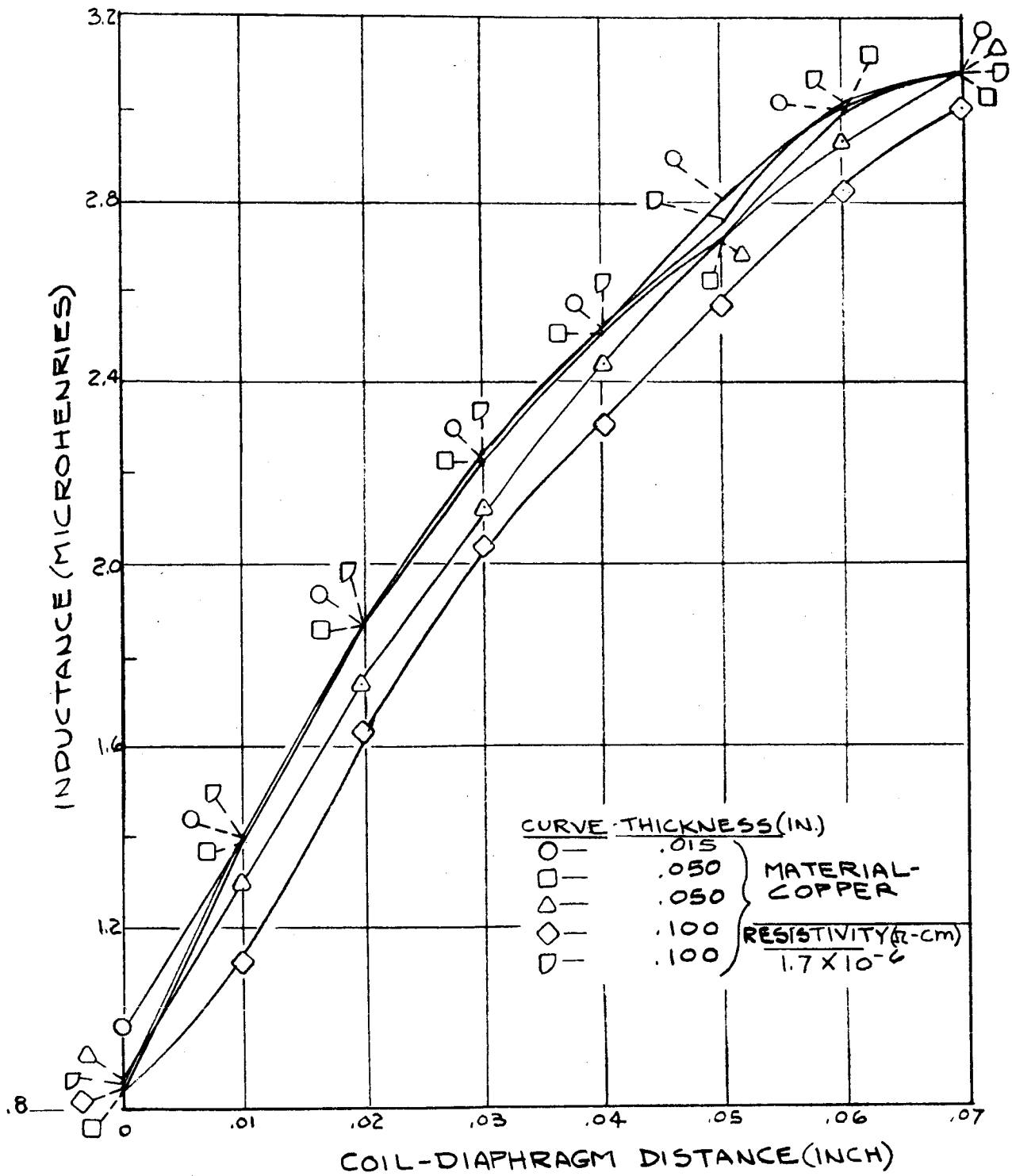


Figure 18

Inductance-Distance Characteristics; Copper Diaphragm

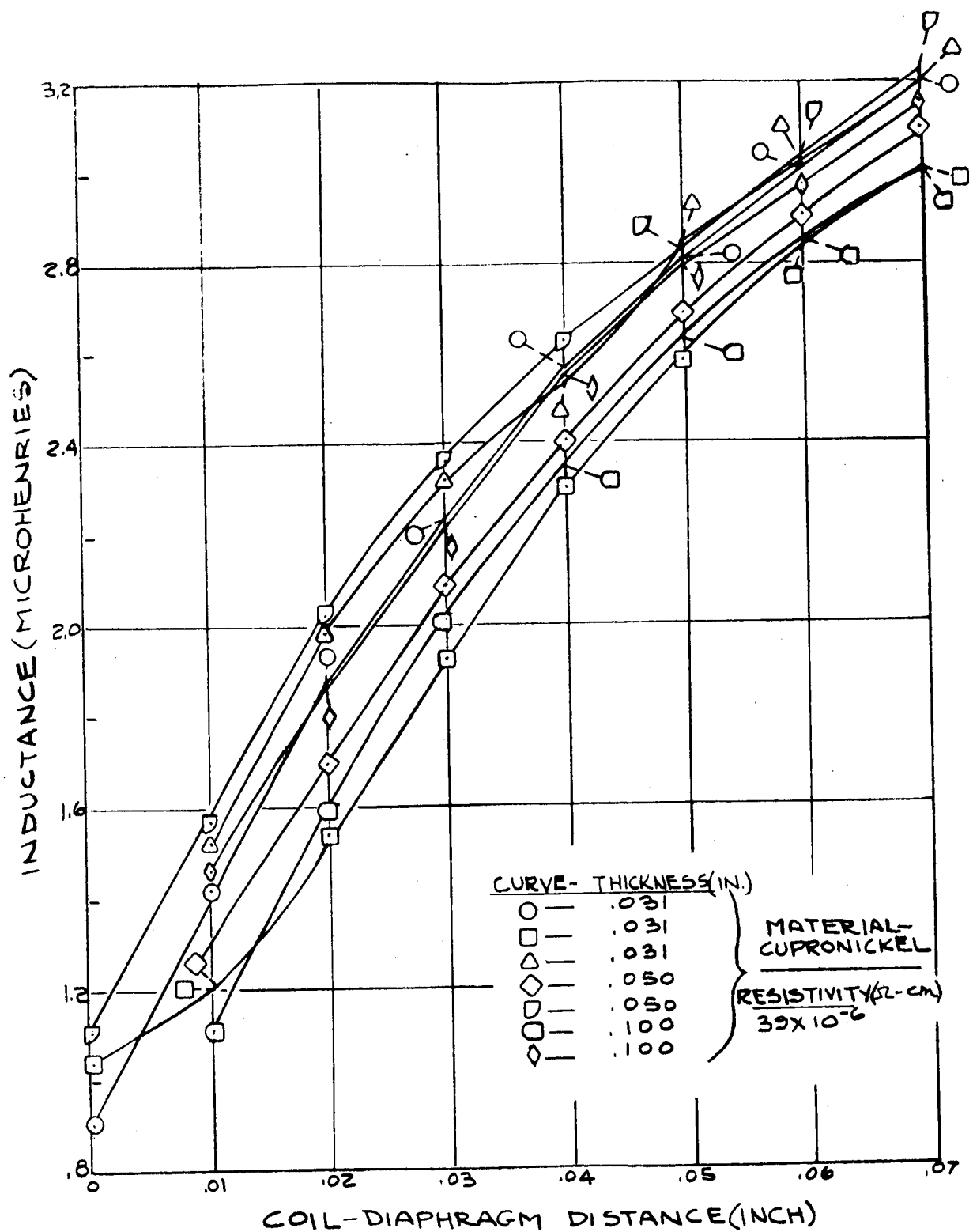


Figure 19

Inductance-Distance Characteristics; Cupronickel Diaphragm

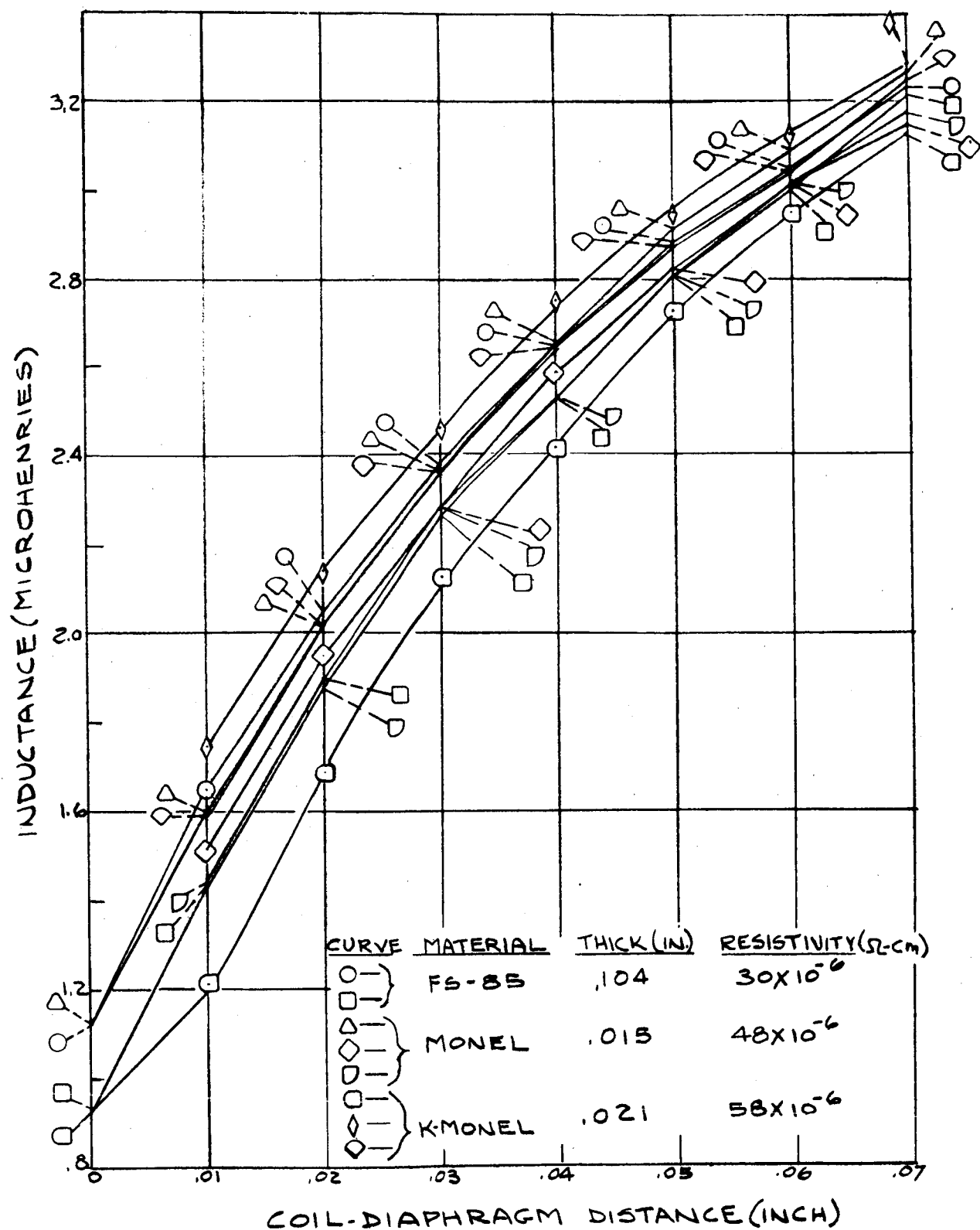


Figure 20

Inductance-Distance Characteristics; FS-85, Monel and K-Monel Diaphragms

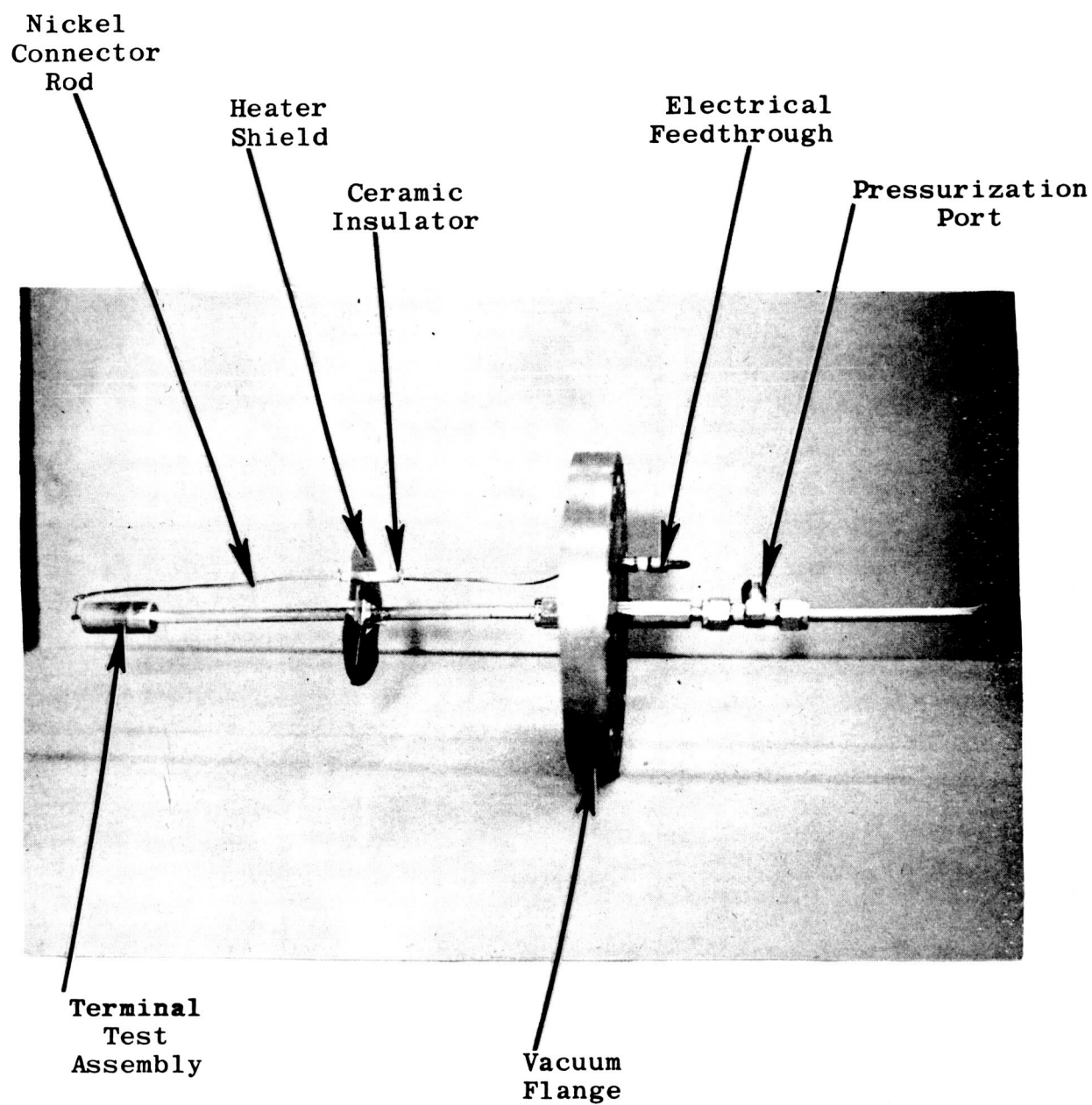


Figure 21
Electrical Terminal Life Test Configuration

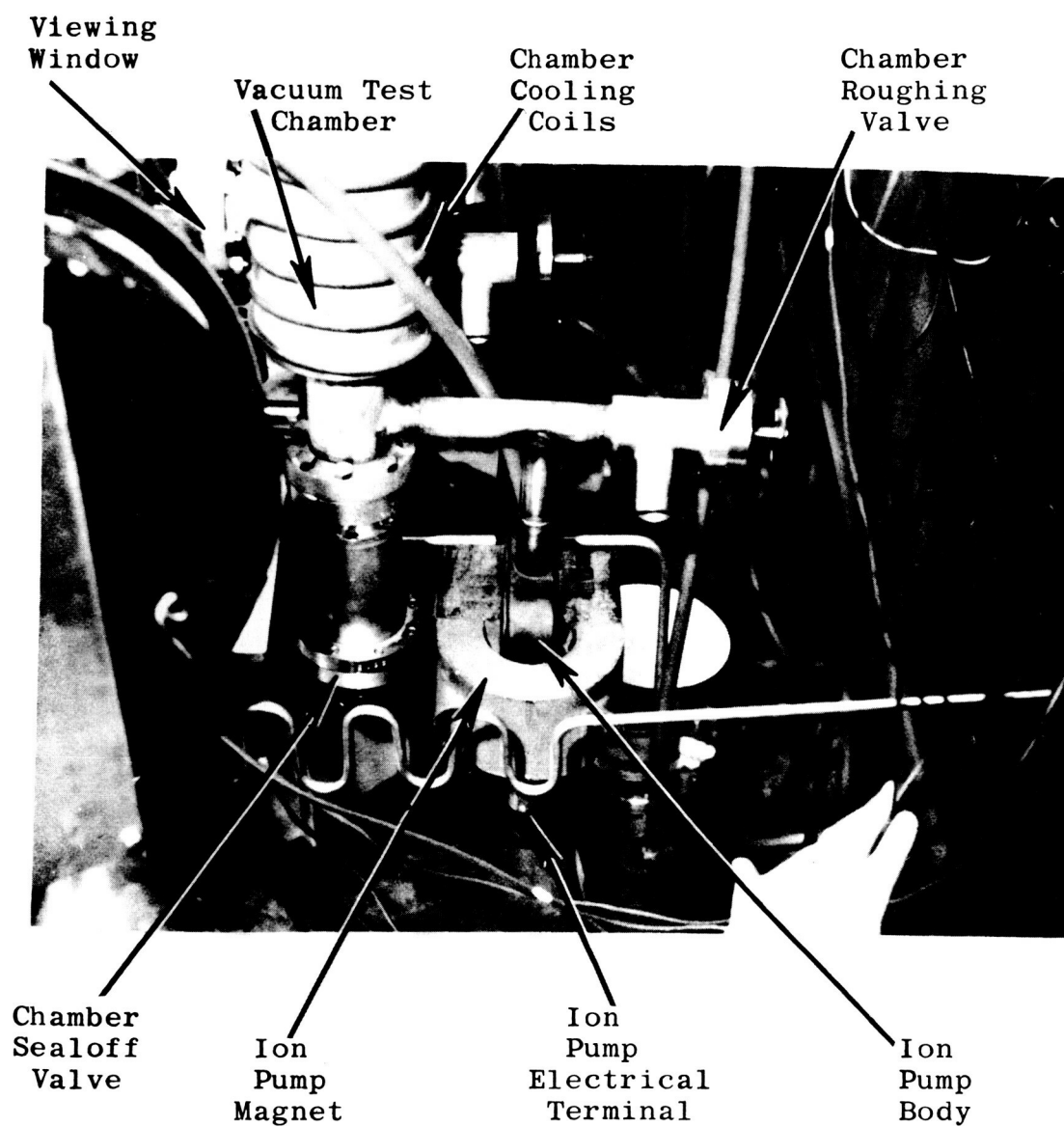


Figure 22
Ion Pump Installation

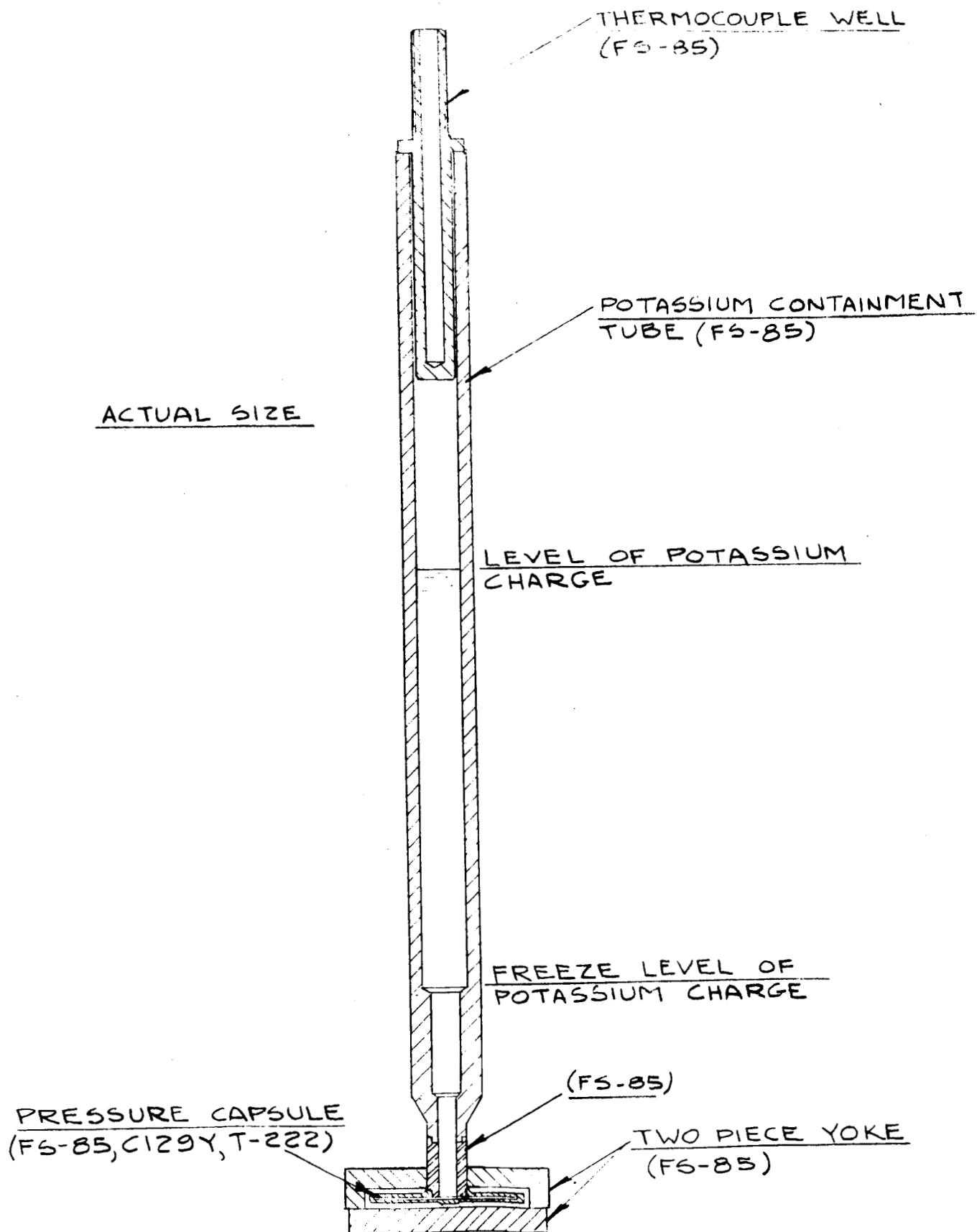


Figure 23

Compatibility Test Design for Columbium and Tantalum Capsules

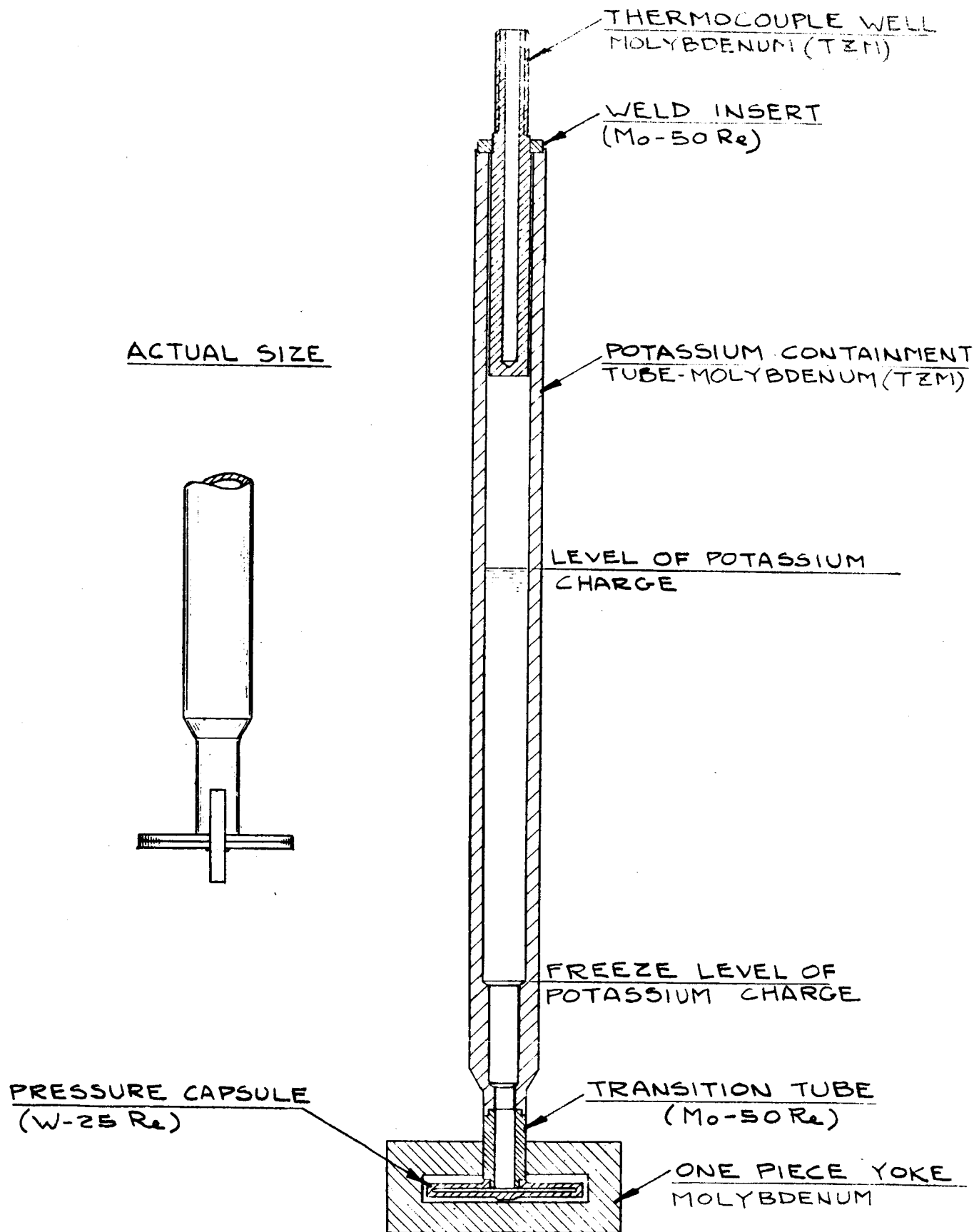


Figure 24

Compatibility Test Design for W-25Re Capsule

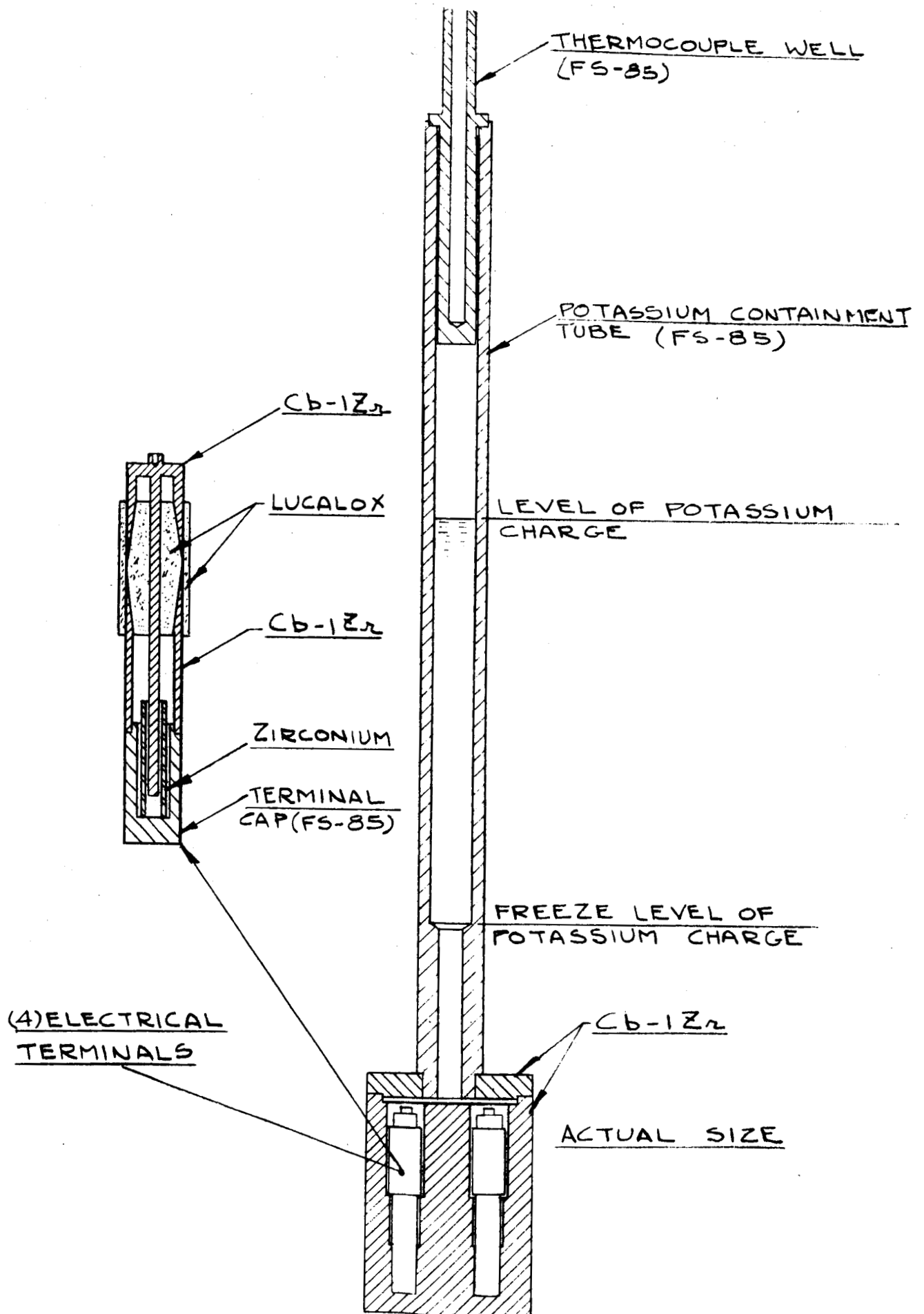


Figure 25

Compatibility Test Design for Electrical Terminals

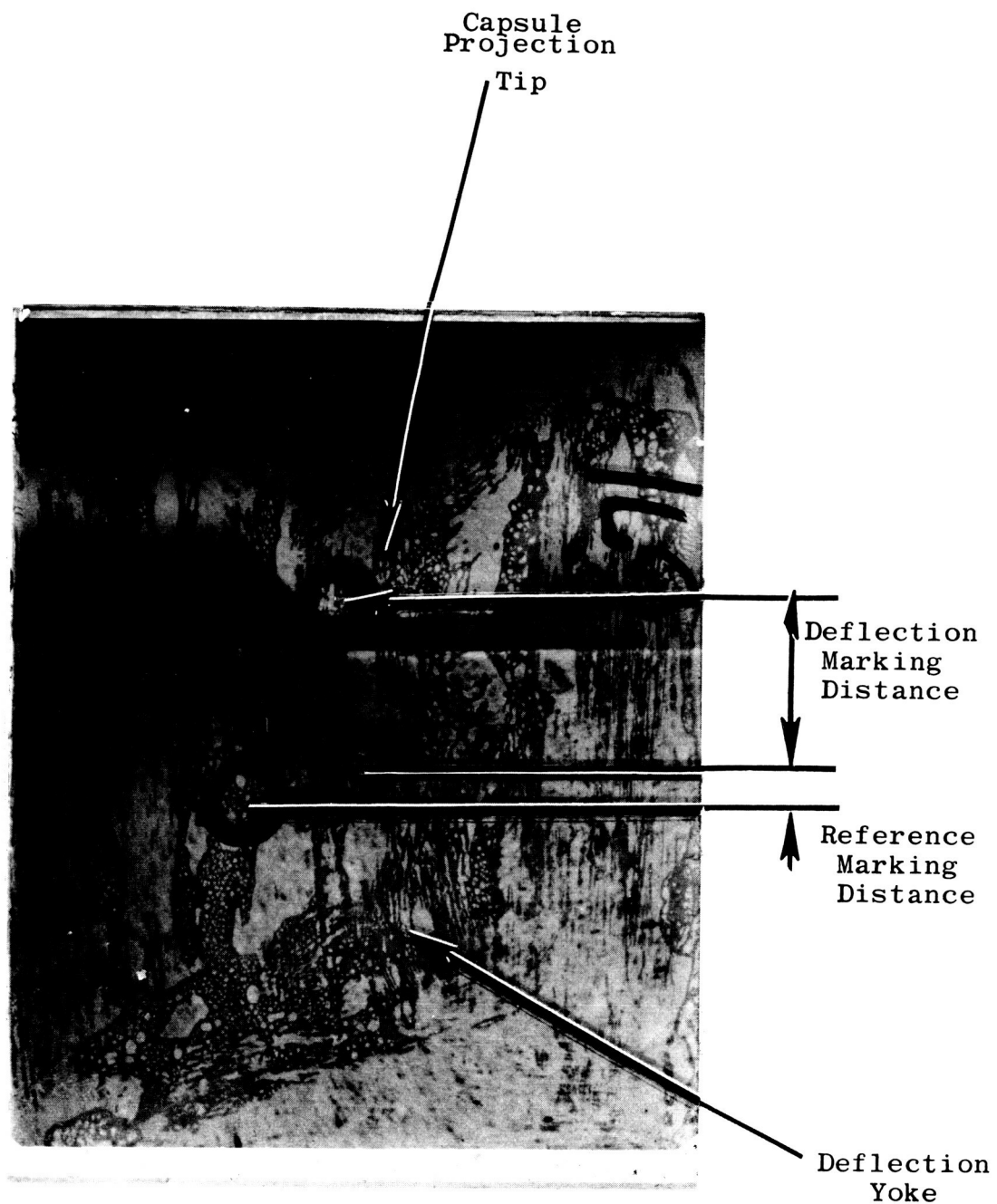


Figure 26
Typical Metallographic Plate

LIST OF REFERENCES

1. R. E. Engdahl, "Second Quarterly Report, Pressure Measuring Systems for Closed Cycle Liquid Metal Facilities", NASA CR-54193, September 28, 1964.

See also:

R. E. Engdahl, "First Quarterly Report, Pressure Measuring Systems for Closed Cycle Liquid Metal Facilities", NASA CR-54140, July 2, 1964.

APPENDIX A

NOMENCLATURE

a	Radius of individual turn of pancake coil
A	Thermionic constant, 120 amperes/cm ² (°K) ²
A _C	Area of capacitor plate
A _e	Thermionic emitter area
B	Thermionic constant
C	Capacitance between pancake coil and diaphragm
C _t	Transmission line capacitance
d	Thermionic emitter-collector distance
d _a	Thermionic emitter - pressure actuated collector distance
d _c	Pancake coil - diaphragm distance
d _r	Thermionic emitter-reference collector distance
e	Electronic charge (1.6 X 10 ⁻¹⁹ coulomb)
E _i	Input voltage to impedance bridge
E _o	Output voltage of impedance bridge
f	Frequency
F.D.	Fineness of detail of objective lens
FL _C	Thermionic collector Fermi level energy

NOMENCLATURE (cont'd)

FL_e	Thermionic emitter Fermi level energy
G_t	Transmission line conductance
H_n	Total axial induction field related to n^{th} turn of pancake coil
H_o	Induction field at center of conductor loop
H_z	Axial induction field component (cylindrical coordinates)
H_ρ	Radial induction field component (cylindrical coordinates)
i_a	Thermionic active collector current
i_o	Pancake coil loop current
i_r	Thermionic reference collector current
I	Thermionic current density
$\mathfrak{F}'_1, \mathfrak{F}'_2$	Elliptic integrals related to pancake coil
$\mathfrak{F}''_1, \mathfrak{F}''_2$	Elliptic integrals related to image coil
I_c	Current density for critical thermionic emitter
I_s	Saturation emission capability of a surface (current density)
J	$\sqrt{-1}$
K	The Boltzmann Constant (1.38×10^{-23} joule/deg.K)

NOMENCLATURE (cont'd)

L	Pancake coil inductance
L _t	Transmission line inductance
m,n	Indexing parameter
n _r	Index of refraction
N	Number of turns in pancake coil
N.A.	Numerical aperture of objective lens
r _i	Inner radius of coaxial cable
r _o	Outer radius of coaxial cable
R _t	Transmission line resistance
s	Distance along transmission line from the input end
S	Transmission line length
S _b	Bartberger factor
t	Time
T	Temperature
T _c	Critical emitter temperature above which space charge occurs
V	Voltage applied to thermionic collector
V _c	Effective emitter-collector potential difference

NOMENCLATURE (cont'd)

V_e	Potential due to thermionic space charge effect
V_m	Voltage generated in individual turn of pancake coil
V_t	Total voltage generated in pancake coil
x_c	Distance from collector to maximum space charge
x_e	Distance from emitter to maximum space charge
X_c	Pancake coil reactance
$2z_e$	Spacing between pancake and image coils
Z_i	Input impedance of transmission line
Z_L	Terminating load impedance of transmission line
Z_o	Characteristic impedance of transmission line
α	Transmission line attenuation constant
β	Transmission line phase constant
γ	Transmission line propagation constant
δ	Skin depth in a medium
δ_e	Skin depth at which field becomes negligible

NOMENCLATURE (cont'd)

ϵ	Dielectric constant of medium =
ϵ_0	Dielectric constant of vacuum (8.854×10^{-12} farad/meter)
ϵ_r	Relative dielectric constant of medium
λ	Wavelength in medium
λ_i	Wavelength of illuminating light
λ_0	Wavelength in vacuum
μ	Permeability of medium =
μ_0	Permeability of vacuum (1.257×10^{-6} henry/meter)
μ_r	Relative permeability of medium
μ_s	Half-angle subtended by objective lens
π	3.1416
ρ_r	Resistivity of material
σ	Conductivity of material
ϕ	Thermionic work factor
ϕ_c	Thermionic collector work function
ϕ_e	Thermionic emitter work function
ϕ_m	Flux linked by individual turn of pancake coil

NOMENCLATURE (cont'd)

ω	Angular frequency - $2\pi f$
(x, y, z)	Cartesian coordinates
(ρ, ϕ, z)	Cylindrical coordinates
(r, θ, ϕ)	Spherical coordinates